




ARTICLE

SORLA is required for insulin-induced expansion of the adipocyte precursor pool in visceral fat

Vanessa Schmidt¹ , Carla Horváth², Hua Dong², Matthias Blüher³, Per Qvist^{4,5} , Christian Wolfrum², and Thomas E. Willnow^{1,4} 

Visceral adipose tissue shows remarkable plasticity, constantly replacing mature adipocytes from an inherent pool of adipocyte precursors. The number of precursors is set in the juvenile organism and remains constant in adult life. Which signals drive precursor pool expansion in juveniles and why they operate in visceral but not in subcutaneous white adipose tissue (WAT) are unclear. Using mouse models, we identified the insulin-sensitizing receptor SORLA as a molecular factor explaining the distinct proliferative capacity of visceral WAT. High levels of SORLA activity in precursors of juvenile visceral WAT prime these cells for nutritional stimuli provided through insulin, promoting mitotic expansion of the visceral precursor cell pool in overfed juvenile mice. SORLA activity is low in subcutaneous precursors, blunting their response to insulin and preventing diet-induced proliferation of this cell type. Our findings provide a molecular explanation for the unique proliferative properties of juvenile visceral WAT, and for the genetic association of SORLA with visceral obesity in humans.

Introduction

Aberrant expansion of white adipose tissue (WAT) mass causes obesity, a pathological condition that is prevalent in populations around the globe (NCD Risk Factor Collaboration [NCD-RisC], 2016; Global BMI Mortality Collaboration et al., 2016). Despite a high degree of functional resemblance, the main WAT depots underneath the skin (subcutaneous [sc]) and in the abdominal cavity (visceral [vis]) are quite distinct in their biological properties and their resulting cardiometabolic risk profiles (Pinnick et al., 2014). While adipogenesis in scWAT is largely confined to the prenatal period, adipogenesis in visWAT proceeds postnatally and contributes to the hyperplastic expansion of this fat depot in a state of energy surplus (Holtrup et al., 2017; Kim et al., 2014; Wang et al., 2013). The adipogenic potential of visWAT is particularly prevalent in the juvenile organism when the size of the adipocyte precursor cell pool in this tissue is determined by nutritional status (Wang et al., 2013). Remarkably, the precursor pool size defined at juvenile age remains constant into adult life (Spalding et al., 2008). Furthermore, recent work demonstrated the importance of these adipocyte progenitor cells in metabolic control (Shao et al., 2018). Still, the signals that promote precursor pool expansion in juveniles and why they operate in visWAT but not in scWAT are important yet unresolved questions.

Sorting-related receptor with A-type repeats (SORL1) is a gene associated with the longitudinal risk of obesity (Smith et al., 2010), i.e., the risk for obesity in adults who were overweight during early childhood (Geserick et al., 2018) or adolescence (reviewed in Singh et al., 2008). SORL1 encodes the type-1 transmembrane protein SORLA (also known as LR11) that acts as an intracellular sorting receptor for the insulin receptor (IR). Specifically, SORLA recycles internalized IR molecules from endosomal compartments back to the cell surface to increase the active surface pool of the IR and to enhance insulin signal reception in target cells (Schmidt et al., 2016). Here, we tested the hypothesis that SORLA activity represents a mechanism linking nutrition through insulin signaling with visceral progenitor cell expansion.

In line with our hypothesis, we document high levels of SORLA expression specific to adipocyte precursors in juvenile visWAT. In these cells, SORLA facilitates signaling by insulin to promote mitotic expansion, a determining step in adipogenesis. In mice lacking SORLA, blunted insulin signaling in response to overfeeding reduces the proliferative capacity of adipocyte precursor cells in juveniles and decreases the progenitor pool size in adults. Contrary to visWAT, this insulin-sensitizing activity of SORLA is absent in precursor cells from scWAT,

¹Max-Delbrueck-Center for Molecular Medicine, Berlin, Germany; ²Laboratory of Translational Nutrition Biology, ETH Zurich, Schwerzenbach, Switzerland; ³Department of Medicine, University of Leipzig, Leipzig, Germany; ⁴Department of Biomedicine, Aarhus University, Aarhus, Denmark; ⁵Centre for Genomics and Personalized Medicine, Aarhus University, Aarhus, Denmark.

Correspondence to Vanessa Schmidt: vanessa.schmidt-krueger@mdc-berlin.de; Thomas E. Willnow: willnow@mdc-berlin.de.

© 2021 Schmidt et al. This article is distributed under the terms of an Attribution–Noncommercial–Share Alike–No Mirror Sites license for the first six months after the publication date (see <http://www.rupress.org/terms/>). After six months it is available under a Creative Commons License (Attribution–Noncommercial–Share Alike 4.0 International license, as described at <https://creativecommons.org/licenses/by-nc-sa/4.0/>).

explaining the distinct proliferative profiles of these two fat depots in response to dietary stimuli.

Results

SORL1 transcript levels in human visWAT but not scWAT correlate with body mass index (BMI)

Previous studies documented that levels of *SORL1* transcript and protein in visWAT are positively correlated with BMI in humans (Schmidt et al., 2016). In mice, overexpression of SORLA in WAT increased adipose tissue mass, while loss of receptor expression protected from diet-induced obesity (Schmidt et al., 2016). While these findings established the relevance of SORLA activity in WAT for body weight control, the mechanism whereby this receptor may affect the longitudinal risk of obesity remained unexplained.

Comparing *SORL1* transcript levels in visWAT and scWAT biopsies in a cohort of 362 adult human subjects, we now show that correlation with BMI is specific for *SORL1* transcript levels in visWAT of males (Fig. 1 A) and females (Fig. 1 B). Surprisingly, this correlation is not seen in scWAT of both sexes (Fig. 1, C and D).

In human WAT, *SORL1* transcripts are found in mature adipocytes with slightly higher levels in vis as compared with sc adipose tissue (Fig. 1 E). Mature adipocytes constitute ~20–40% of the total cell numbers in human WAT (Eto et al., 2009; Miao et al., 2020; Sun et al., 2020). Based on deposited single-cell RNA sequencing (scRNAseq) data (Vijay et al., 2020), the remaining stromal vascular fraction (SVF) of human WAT is composed of adipocyte precursor cells and various immune and endothelial cell types, with adipocyte precursors being more abundant in visWAT as compared with scWAT (76% versus 35% of SVF cells; Fig. 1 G). In the SVF, *SORL1* transcripts are found in precursors and immune cell types at comparable levels (Fig. 1 F). However, whereas adipocyte precursors constitute the main SVF cell type in visWAT to express *SORL1* (77% of cells), few precursors in scWAT express the receptor (3% of cells; Fig. 1 H). This striking observation suggests *SORL1* expression as a feature discriminating adipocyte precursors in human visWAT from those in scWAT.

SORLA is required for diet-induced cell proliferation in visWAT of juvenile mice

A distinctive characteristic of juvenile visWAT is the ability to expand its inherent pool of precursor cells, facilitating hyperplastic growth of this tissue mass in adult life (Wang et al., 2013). To query the contribution of SORLA to precursor cell proliferation, we compared the proliferative capacity in sc inguinal and epididymal (ep) fat pads of mice, either WT or genetically deficient (knockout [KO]) for *Sorl1* (Andersen et al., 2005; Schmidt et al., 2016). Although the precise anatomical localization of these fat pads differs from that in humans, these murine tissues are commonly accepted model systems for human sc and vis fat (Cinti, 2012; Jeffery et al., 2016).

Initially, we studied mice on a normal chow diet at 5 wk (juvenile) or 10 wk (adult) of age. To determine the number of proliferative cells in WAT depots, we quantified EdU⁺ (5-ethynyl-2'-deoxyuridine) cells in these mice following supplementation with EdU in drinking water for 7 d (Jeffery et al., 2015). In

WT mice, proliferative (EdU⁺) cells were detected in epWAT and scWAT in the adult (Fig. 2, A and C) and in the juvenile stage (Fig. 2, B and C). However, the proliferative capacity was highest in juvenile epWAT, exceeding that of other juvenile or adult fat tissues by fourfold (Fig. 2 C). SORLA deficiency decreased the number of EdU⁺ cells in epWAT and scWAT of KO mice, documenting the relevance of receptor activity for cell proliferation in these tissues (Fig. 2 C). To specifically investigate the impact of SORLA on nutrition-induced cell proliferation, we fed juvenile mice a high-fat diet (HFD) for 3 d and quantified the resulting numbers of proliferating cells in WAT thereafter using EdU incorporation. In juvenile WT animals, short-term HFD feeding increased the number of EdU⁺ cells in epWAT by fivefold as compared with normal chow feeding (Fig. 2 D). This substantial increase in proliferating cells was not seen in juvenile scWAT, or in epWAT and scWAT from adult WT mice (Fig. 2 D). This diet-induced increase in cell proliferation in epWAT was significantly reduced in juvenile mice lacking SORLA (Fig. 2 E). By contrast, no effect of SORLA deficiency on HFD-induced cell proliferation was seen in scWAT (Fig. 2 F). Thus, while SORLA deficiency impairs basal levels of cell proliferation in scWAT and epWAT to a similar extent, its impact on nutrient-induced cell proliferation is unique to juvenile epWAT, and not seen in scWAT.

SORLA increases the proliferative capacity of adipocyte precursor cell types in juvenile epWAT but not scWAT

Quantification of EdU⁺ cells by immunohistology (as in Fig. 2) encompassed adipocyte precursors but also other proliferating cell types in the murine WAT potentially impacted by receptor deficiency. Thus, we refined further analysis by focusing on adipocyte precursors isolated from these tissues. To do so, we applied a multicolor FACS scheme to isolated a (Lin⁻CD29⁺CD34⁺Sca1⁺) cell population that constitutes the early adipocyte precursor cell type in WAT. This precursor cell population can be further distinguished into adipocyte progenitors (CD24⁺) and committed preadipocytes (CD24⁻; Berry and Rodeheffer, 2013; Rodeheffer et al., 2008). Both cell populations express Pdgfr α , a marker of the adipogenic lineage (Berry and Rodeheffer, 2013). Here, we applied multicolor FACS to characterize these two precursor cell populations in epWAT and scWAT of juvenile WT and KO mice (Fig. S1, A–D).

Sca1⁺ adipocyte precursors express SORLA as documented by quantitative RT-PCR and Western blotting (Fig. 3 A). *Sorl1* transcript levels were highest in precursors from juvenile epWAT as compared with adult epWAT (3-fold) or juvenile or adult scWAT (7- or 15-fold; Fig. 3 B). The proliferative capacity of CD24⁺ progenitors and CD24⁻ preadipocytes in juvenile epWAT was significantly reduced by SORLA deficiency as shown by treating WT and KO mice with BrdU and by subsequent quantification of BrdU⁺ cells in the sorted Sca1⁺ cell populations (Fig. S1 E and Fig. 3 C). No impact of SORLA deficiency on the proliferative capacity of progenitors or preadipocytes was seen in scWAT (Fig. 3 D). Impaired precursor cell proliferation coincided with a significant reduction in the number of CD24⁺ progenitors in epWAT (Fig. 3 E) but not in scWAT (Fig. 3 F) of juvenile KO mice. This fat depot-specific impact of SORLA deficiency on the proliferative capacity of Sca1⁺ precursors in

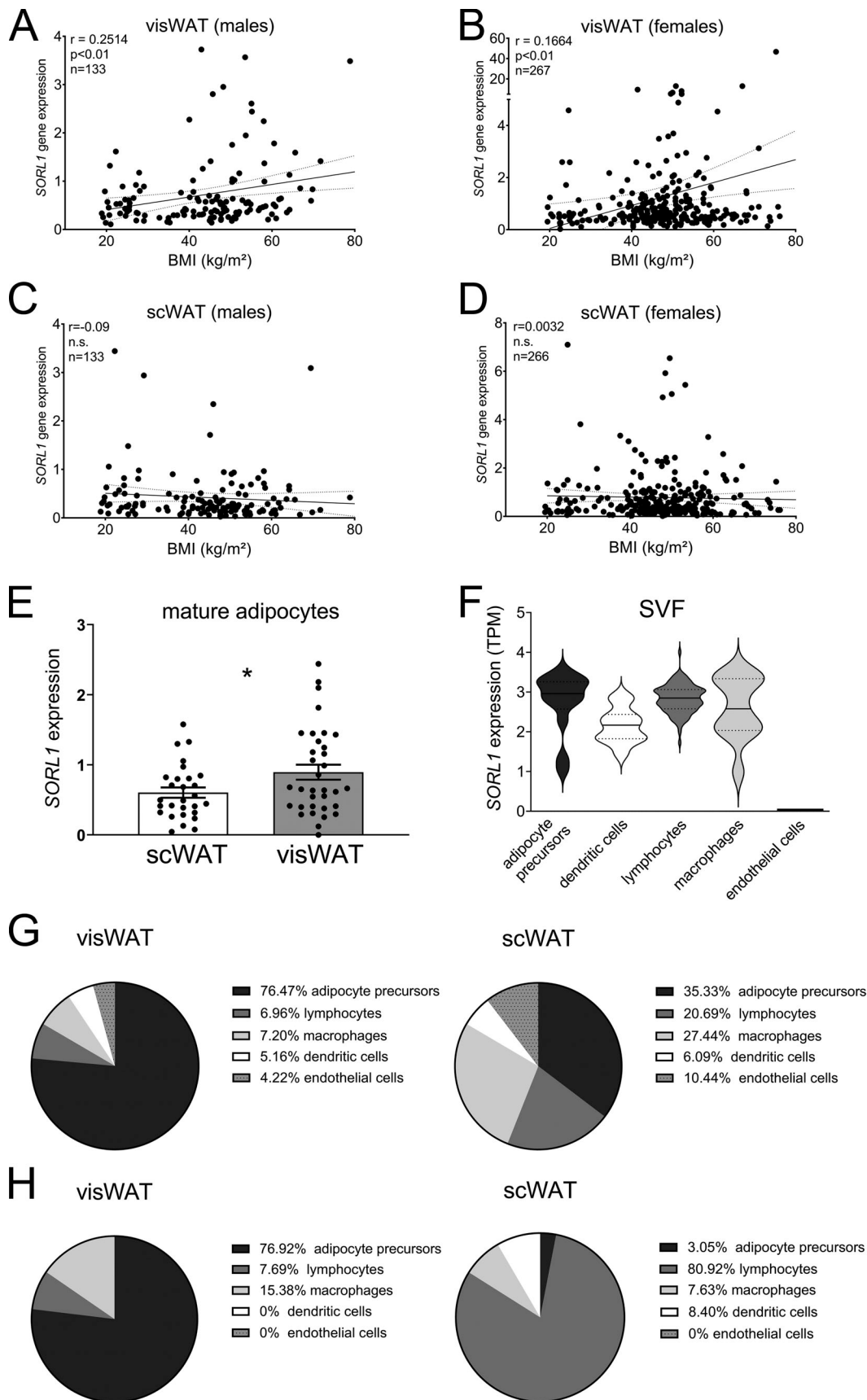


Figure 1. **SORL1** transcript levels in vis but not sc human WAT correlate with BMI. (A–D) Levels of *SORL1* transcripts were determined by quantitative RT-PCR in human vis and scWAT samples and calculated as relative to levels of 18S rRNA in the samples. Correlation of *SORL1* transcript levels with BMI is seen in

visWAT of males (A, $n = 133$) and females (B, $n = 267$), but not in scWAT of both sexes (C, $n = 133$; and D, $n = 266$). Significance of data was determined using linear regression analysis with Pearson correlation coefficient. (E) Levels of *SORL1* transcripts in mature adipocytes were determined by quantitative RT-PCR in human vis and scWAT samples and calculated relative to levels of 18S rRNA in the respective sample. Data are given as mean \pm SEM ($n = 28$ for scWAT, $n = 34$ for visWAT). Statistical significance of data were determined using two-sided Student's *t* test; *, $P < 0.05$. (F) *SORL1* transcript abundance (transcripts per million [TPM]) in SVF cell types of human WAT. (G) Percent distribution of cell types in the SVF of human scWAT and visWAT. (H) Percent distribution of cell types in the SVF of human scWAT and visWAT among *SORL1*-expressing cells. Data in F–H are based on deposited single-cell RNA sequencing data (Vijay et al., 2020).

epWAT, but not scWAT, was also seen in juvenile mice fed an HFD for 1 wk (Fig. 3 G). Apart from an apparent decrease in the number of adipocyte precursors in mutant epWAT, *SORL1* deficiency did not cause any discernable alteration in the numbers of various immune and endothelial cell types in the sorted SVF of epWAT or scWAT (Fig. S2).

SORLA promotes proliferation of epididymal adipocyte precursor cells by a cell-autonomous mechanism

In mature adipocytes, *SORLA* acts as a transmembrane receptor to promote functional expression of the IR (Schmidt et al., 2016). However, *SORLA* in adipocytes is also subject to ectodomain shedding, releasing the extracellular portion of the receptor that

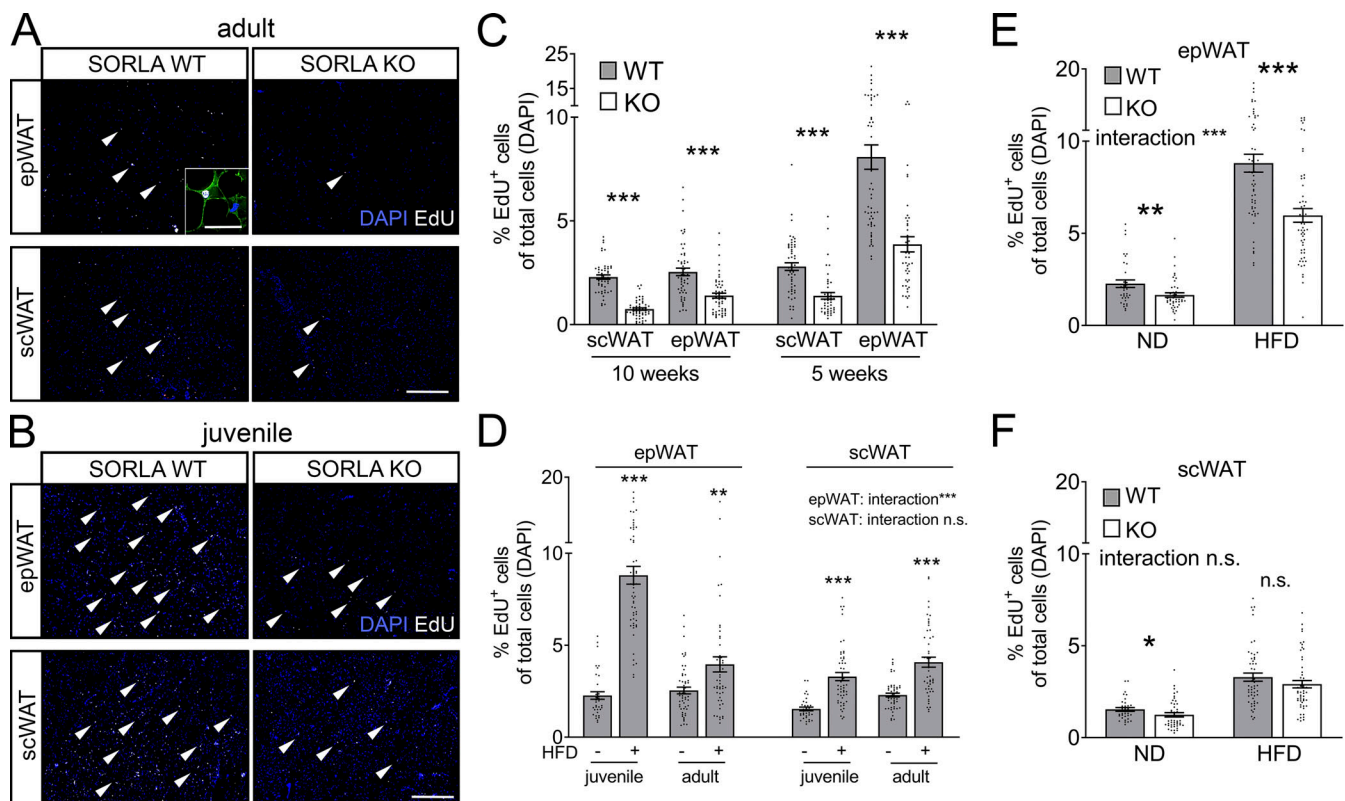


Figure 2. SORLA defines the nutrient-dependent proliferative capacity of epWAT of juvenile mice. (A) Immunodetection of EdU⁺ cells on 15 μ m sections of ep and scWAT of adult WT and *SORLA* KO mice at 10 wk of age (7 d of EdU dosing). Exemplary EdU⁺ cells (white signals) are marked with arrowheads. Cells were counterstained with DAPI (blue). The high-magnification inset shows an EdU⁺ cell stained for adipocyte marker perilipin (green). (B) Data as for A but from juvenile WT and KO mice at 5 wk of age. Scale bars in A and B: 200 μ m (inset: 85 μ m). (C) Quantifications of EdU⁺ cells (percentage of DAPI⁺ cells) in epWAT and scWAT of adult or juvenile WT and *SORLA* KO mice on a normal chow are shown. Identical numbers of DAPI⁺ cells were scored for both genotypes in the respective age group (adults: 13,500 for scWAT and 7,000 for epWAT; juveniles: 41,000 for scWAT and 24,000 for epWAT). Data are given as mean \pm SEM from $n = 6$ animals per genotype (three histological sections per animal, three images per section). Two-sided Student's *t* test; ***, $P < 0.001$. (D) Juvenile or adult WT animals were fed a normal chow (-) or an HFD (+) for 3 d (juvenile) or 7 d (adult) while being exposed to EdU in drinking water. Subsequently, the number of EdU⁺ cells (percentage of total DAPI⁺ cells) was scored on immunohistological sections of epWAT and scWAT samples. Data are the mean \pm SEM from $n = 5$ or 6 animals per genotype (three histological sections per animal, three images per section). The significance of data were determined using two-way ANOVA and Sidak's multiple comparisons test; **, $P < 0.01$; ***, $P < 0.001$. The HFD-induced increase in cell proliferation was significantly higher in epWAT of juvenile mice as compared with adult animals or to juvenile or adult scWAT (interaction for epWAT, ***, $P < 0.001$; interaction for scWAT, not significant). (E and F) Juvenile WT or KO mice were fed a normal chow (ND) or an HFD for 3 d while being exposed to EdU in drinking water. Subsequently, the number of EdU⁺ cells (percentage of total DAPI⁺ cells) was scored on immunohistological sections of ep (E) and sc (F) WAT samples. Data are the mean \pm SEM from $n = 5$ or 6 animals per genotype (three histological sections per animal, three images per section). The significance of data was determined using two-sided Student's *t* test; *, $P < 0.05$; **, $P < 0.01$; ***, $P < 0.001$. In juvenile epWAT, the HFD-induced increase in cell proliferation was significantly lower in KO as compared with WT mice (two-way ANOVA for interaction; ***, $P < 0.001$ and Sidak's multiple comparisons test). No effect of *SORLA* genotype on HFD-induced EdU⁺ counts was seen in scWAT. Identical numbers of DAPI⁺ cells were scored for both genotypes (1,700 for scWAT; 1,500 for epWAT). A normal distribution of data were assumed in C–F, but this was not formally tested.

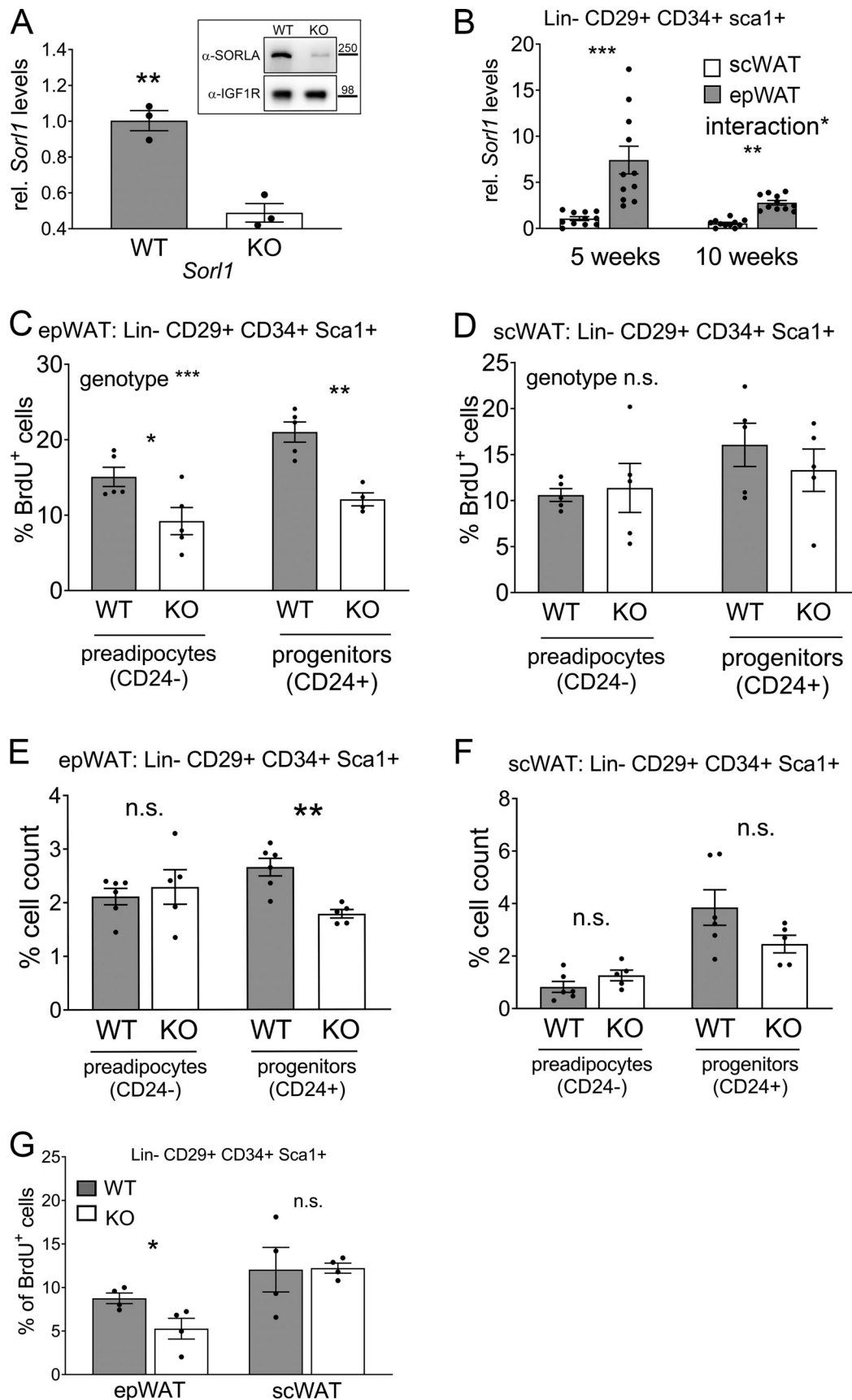


Figure 3. **SORLA increases the proliferative capacity and the number of early adipocyte precursor cells in juvenile epWAT.** (A) Levels of *Sor1* transcripts and SORLA protein (inset) in Sca1⁺ adipocyte precursors from WT and SORLA KO adipose tissues were determined by qPCR and Western blotting,

respectively. Detection of IGF1R served as loading control for Western blot analysis. Data are given as mean \pm SEM relative to WT levels (set to 1). Statistical significance of data was determined using two-sided Student's *t* test ($n = 3$ independent samples per genotype for qPCR, 5 or 6 samples per genotype for Western blotting). **, $P < 0.005$. Numbers to the right of the blots are in kilodaltons. **(B)** Levels of *Sorl1* transcripts as determined by qPCR in sc and epWAT of 5-wk-old or 10-wk-old WT mice. Levels are given as relative to scWAT at 5 wk of age. *Sorl1* transcript levels are significantly higher in epWAT than in scWAT, a difference most pronounced in juveniles. Statistical significance of data (mean \pm SEM; $n = 11$) was determined using paired Wilcoxon test as well as two-way ANOVA for interaction; *, $P < 0.01$; for tissue, ***, $P < 0.001$; for age, **, $P < 0.01$. **(C and D)** Quantification of BrdU⁺ cells in subpopulations of Sca1⁺ adipocyte precursors sorted from epWAT (C) and scWAT (D) of juvenile mice of the indicated genotypes. Previously, animals had received BrdU in drinking water for 3 d. The numbers of proliferating (BrdU⁺) precursor cell types are significantly higher in epWAT of WT as compared with KO animals (C). No statistically significant differences in (BrdU⁺) precursor cell numbers are seen in scWAT comparing genotypes (D). Data are the mean \pm SEM. Two-way ANOVA and Sidak's multiple comparisons test; *, $P < 0.05$; **, $P < 0.01$; ***, $P < 0.001$ ($n = 5$ animals per genotype). **(E and F)** Number of Lin⁻CD34⁺CD29⁺Sca1⁺ cell types in epWAT (E) and scWAT (F) of juvenile WT and KO mice was quantified on the basis of CD24 expression. The number of CD24⁺ progenitors in epWAT is significantly higher in juvenile WT as compared with KO mice (E). No statistically significant differences in CD24⁺ adipocyte progenitors are seen in scWAT comparing genotypes (F). Data show the mean \pm SEM 100,000 cells per animal were analyzed. Statistical significance of data ($n = 5$ or 6 animals per genotype) was determined using two-sided Mann-Whitney test. **, $P < 0.01$. **(G)** Juvenile WT or KO animals were set on an HFD and treated with BrdU in drinking water for 7 d. Subsequently, Lin⁻CD34⁺CD29⁺Sca1⁺ cell types in epWAT and scWAT were sorted and numbers of BrdU⁺ cells quantified. BrdU⁺ adipocyte precursors in epWAT are significantly higher in juvenile WT as compared with KO mice. No statistical significant differences in BrdU⁺ adipocyte precursor numbers in scWAT are seen comparing genotypes. Data show the mean \pm SEM of four animals per genotype. Statistical significance of data was determined using two-sided Mann-Whitney test. *, $P < 0.05$. A normal distribution of data was assumed in A, C, and D, but this was not formally tested.

acts as a paracrine factor in control of thermogenic gene expression (Whittle et al., 2015). To query whether SORLA promotes nutrient-induced proliferation of adipocyte precursors mainly through a cell-autonomous or a non-cell-autonomous mechanism, we performed cell transplantation experiments in mice (Fig. 4 A). In detail, we purified the Sca1⁺ precursor cell population from SVF of the epWAT of juvenile mice and transplanted them into the scWAT pad of recipient animals using Matrigel plugs (Schwalie et al., 2018). Subsequently, we treated the recipients with an HFD for 5 wk and with EdU in drinking water for the first 2 wk of the protocol. Finally, we quantified the number of EdU⁺ cells in the Matrigel plugs recovered from the recipients using immunohistology (Fig. 4 B). Dissection was meant to assure that mainly transplanted cells were quantified,

although infiltration of some host cells into the Matrigel plug could not be excluded. In these transplantation experiments, WT precursors from epWAT showed a robust proliferative capacity when introduced into the scWAT of WT recipients (68% EdU⁺ cells; Fig. 4 C, WT in WT). WT precursors showed a comparable proliferative capacity when transplanted in scWAT of KO recipients (59% EdU⁺ cells; Fig. 4 C, WT in KO). By contrast, the number of proliferating cells was significantly lower when epWAT precursors from KO donors were implanted into the scWAT of KO recipients (41% EdU⁺ cells; Fig. 4 C, KO in KO). Although transplanting these cells into the scWAT of WT recipients improved their proliferative capacity (51% EdU⁺ cells; Fig. 4 C, KO in WT), this increase was not statistically significant when compared with the KO in KO condition. This observation

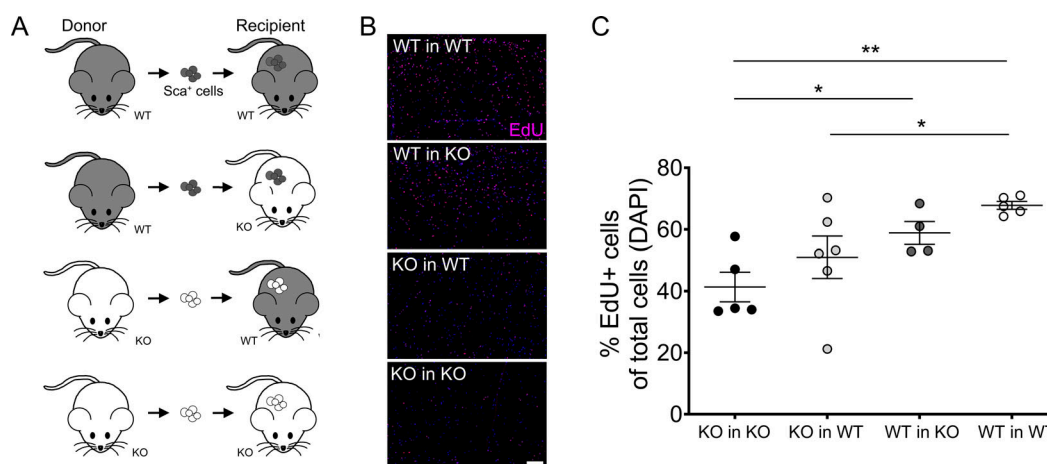


Figure 4. **SORLA promotes the proliferative capacity of adipocyte precursor cells in vivo by a cell-autonomous mechanism.** **(A)** Strategy of adipocyte precursor cell transplantation experiments. The Sca1⁺ adipocyte precursor cells from the SVF was isolated from the epWAT of juvenile donor mice and transplanted into the scWAT pad of adult recipients using Matrigel plugs. Mice had the indicated SORLA genotypes. Subsequently, recipients received 2 wk EdU in drinking water to label proliferative cells and were set on an HFD for 5 wk to induce precursor cell proliferation in the transplanted Matrigel plugs. **(B)** Exemplary histological sections of transplanted tissue pads of the indicated transplantation experiments coimmunostained for EdU (purple) and DAPI (blue). Scale bar: 100 μ m. **(C)** The number of proliferating (EdU⁺) cells in transplanted tissue pads in the indicated transplantation experiments was determined and pooled on three histological sections of four to six mice per genotype and condition and given as percentage of total DAPI⁺ cells in the section. Counted cells: 69,000 (KO in KO); 102,000 (KO in WT); 61,000 (WT in KO); 71,000 (WT in WT). Data are the mean \pm SEM. Two-sided Mann-Whitney test; *, $P < 0.05$; **, $P < 0.01$.

argued that a cell-intrinsic mechanism of SORLA action plays an important role in diet-induced precursor cell proliferation.

SORLA is required for insulin-dependent mitotic expansion of adipocyte precursors

Murine embryonic fibroblasts (MEFs) are a well-established model to study mechanisms of adipogenesis (Ruiz-Ojeda et al., 2016). When treated with an induction cocktail containing insulin, rosiglitazone, 3-isobutyl-1-methylxanthine, and dexamethasone, MEFs recapitulate an adipogenic program that entails synchronous entry of progenitors into cell cycle, followed by several rounds of mitosis (mitotic expansion). The resulting committed preadipocytes undergo differentiation to mature adipocytes as evidenced by expression of adipocyte-specific genes and by lipid filling.

We compared the adipogenic potential of MEFs derived from WT or SORLA KO mice to dissect the exact step in which SORLA promotes adipogenesis. After 7 d of differentiation, Oil Red O staining for lipids was substantially reduced in KO MEF cultures compared with WT (Fig. 5, A and B). We also observed a strong decrease in expression of mature adipocyte markers using Western blotting (Fig. 5, C and D) and quantitative RT-PCR analysis (Fig. S3 D), indicating reduced numbers of adipocytes being produced in the absence of SORLA. To delineate whether these changes were due to defects in cell differentiation, we analyzed expression of markers of early CCAAT/enhancer binding protein (Cebp) Δ and β (*Cebpd*, *Cebpb*) and later *Cebpa* stages of differentiation. Marker levels were comparable between the two genotypes (Fig. S3, A–C), arguing that the reduced lipid accumulation in KO MEF cultures was not due to an impairment in adipocyte maturation from committed preadipocytes.

Multiple signaling pathways are involved in generation of mature adipocytes from progenitors, including signaling through IR (Suryawan et al., 1997) and insulin-like growth factor 1 receptor (IGF1R; Smith et al., 1988), as well as through downstream MAPK and PI3K/protein kinase B (AKT) pathways (Liu et al., 2015; Moseti et al., 2016). Therefore, we compared the levels of pathway components of these differentiation programs in SORLA WT and SORLA KO MEFs treated with the induction cocktail. Prior to treatment, the total levels of IR and IGF1R, as well as of AKT, extracellular-signal regulated kinase (ERK), mitogen-activated protein kinase kinase 4 (MKK4), and JNK, were identical in both genotypes (Fig. S3, E and F). Also, the levels of phosphorylated (active) forms of pAKT, pERK, and pJNK were unchanged, while levels of pMKK4 were slightly increased in SORLA KO MEFs (Fig. S3, E and F). However, 5 min after addition of the induction cocktail, KO MEFs failed to show a robust increase in phosphorylation (i.e., activation) of several pathway components, including pIR, pIGF1R, pAKT, pERK, pMKK4, and pJNK that was readily observed in WT cells (Fig. 5, E and F).

An initial step in adipogenesis entails mitotic expansion of progenitors (Reichert and Eick, 1999). Progression through several rounds of mitosis is coordinated by key regulators of the cell cycle including cyclins D1 and E1 (Baldin et al., 1993) as well as transcription factors FOXO1a and 3a (Schmidt et al., 2002). Levels of cyclin D1, cyclin E1, and FOXO1a/3a were comparable

in WT and KO MEF preparations before induction as shown by quantitative Western blot analysis (Fig. 6, A and B). However, 10 min after addition of the induction cocktail, a failure to increase levels of these proteins was evident in KO MEFs as compared with WT cells (Fig. 6, C and D). In line with impaired induction of MAPK and PI3K/AKT pathways and cell cycle regulators, stimulated KO MEFs failed to initiate robust cell proliferation as documented by EdU incorporation (Fig. 6, E and F). By contrast, pronounced cell proliferation was evident in MEFs derived from WT mice following treatment with the induction medium (Fig. 6, E and F).

Levels of SORLA activity define the ability of adipocyte precursors to respond to mitogenic stimuli from insulin

We substantiated the necessity of SORLA for insulin-induced adipogenesis in the SVF isolated from murine WAT. In agreement with data obtained in MEFs, SVF cells from juvenile epWAT of KO mice failed to increase pIR, pERK, and pJNK levels to the same extent as WT cells following application of induction medium (Fig. 7, A and B, time point 5 min). No difference in baseline levels of pERK and pJNK was observed in the SVF of juvenile epWAT before induction (Fig. 7, A and B, time point 0 min). Importantly, no impact of SORLA deficiency on insulin pathway stimulation (i.e., pIR, pERK, or pJNK levels) was observed in cells isolated from scWAT of juvenile mice (Fig. 7, A and B, time point 5 min). The tissue type-specific action of SORLA in epWAT was confirmed by quantifying cell proliferation using EdU incorporation. Following application of induction medium, the proliferative capacity of SVF cells from epWAT of juvenile KO mice was significantly lower than that of cells from juvenile WT epWAT (Fig. 7 C). No impact of SORLA activity on proliferation was observed comparing cells isolated from scWAT of WT or KO mice (Fig. 7 D). In line with a decreased proliferative capacity, we observed reduced transcript levels for adipocyte differentiation markers cEBP α , LPL, and FABP4 in SVF preparations from KO as compared with WT epWAT 1 wk after treatment with induction medium (Fig. 7 E). No difference in adipocyte marker gene expression was observed comparing SVF from scWAT of WT and KO animals (Fig. 7 F). To corroborate that SORLA specifically impacted the cellular response to insulin, we treated the SFV from epWAT with induction cocktails containing or lacking this hormone. A substantial increase in pIR and pAKT levels in WT cells was only seen with the full cocktail (w/) but not with induction medium lacking insulin (w/o; Fig. 7, G and H). Insulin action on pIR and pAKT levels was blunted in the SVF from KO epWAT treated with the full induction cocktail (Fig. 7, G and H).

To ultimately document the necessity of SORLA for insulin-dependent proliferation and differentiation of adipocyte precursor cells, we repeated the differentiation experiment in flow-sorted Sca1⁺ precursors from juvenile WAT. In agreement with the results obtained in the SVF, Sca1⁺ cells from juvenile KO epWAT failed to increase pIR, pAKT, and pERK levels to the same extent as WT cells following application of induction medium for 5 min (Fig. 8, A and B, stimulated). No difference in baseline levels of pAKT and pERK was observed before induction (Fig. 8, A and B, unstimulated). By contrast, no insulin-induced

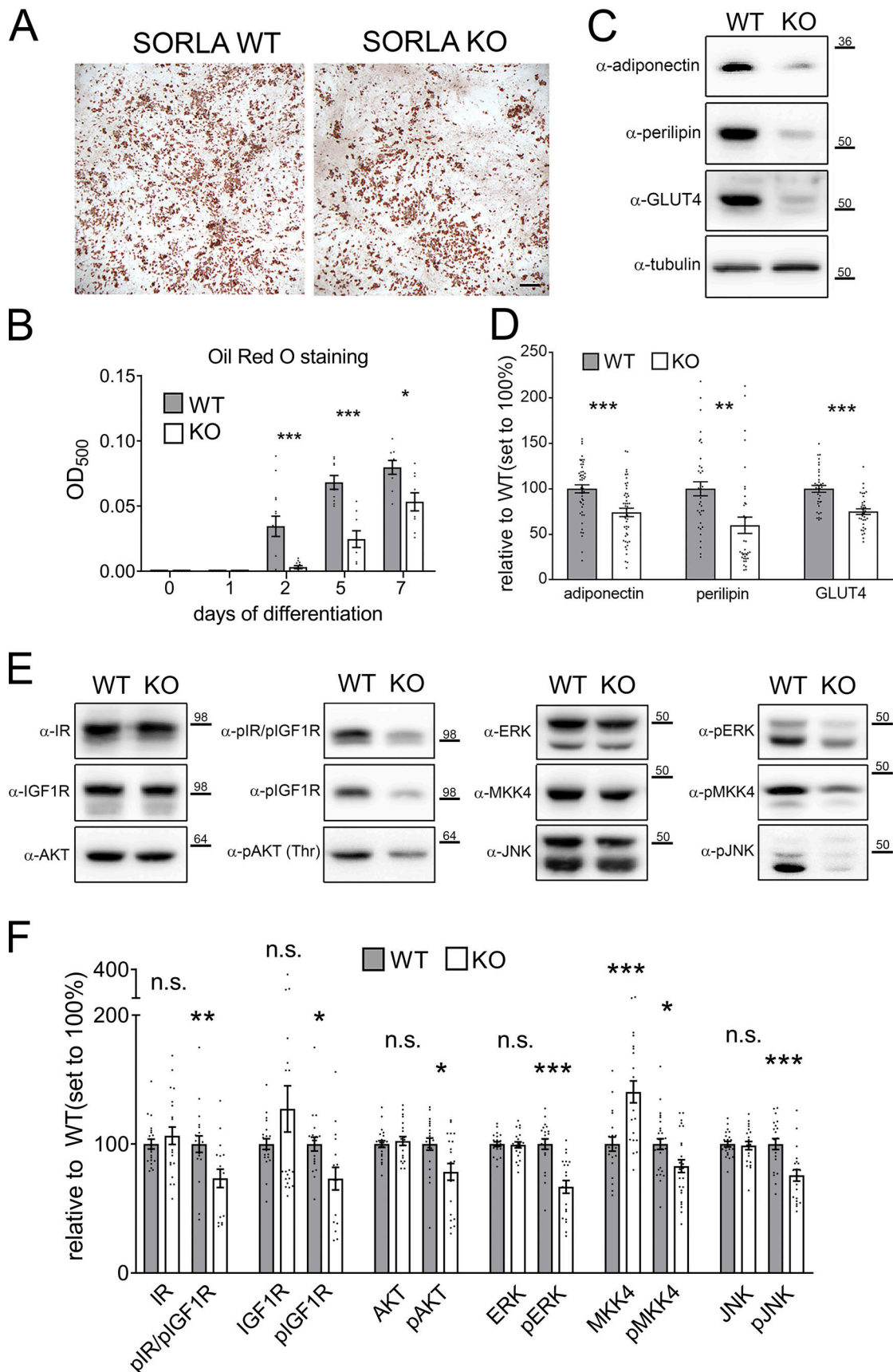


Figure 5. **SORLA promotes insulin-induced generation of mature adipocytes from MEFs.** (A and B) MEFs from WT and SORLA KO mice were differentiated for 7 d, and the extent of adipogenesis was scored by lipid staining (Oil Red O staining). Exemplary images at day 7 (A) and quantification of lipid filling

(B) of replicate differentiation experiments ($n = 9$ or 10) over time of differentiation are shown. Data are the mean \pm SEM. Scale bar in A: 500 μm . (C and D) Western blot analysis of levels of the indicated markers in mature adipocytes differentiated from WT and SORLA KO MEFs. Exemplary Western blots (C) and densitometric scanning of replicate blots (D; $n = 35$ – 49 individual samples) are shown. Expression levels in D are given as relative to WT (set to 100%). Data are shown as mean \pm SEM. Significance of data was evaluated by two-way ANOVA and Sidak's multiple comparisons test (B) or two-sided Student's t test (D). *, $P < 0.05$; **, $P < 0.01$; ***, $P < 0.001$. (E and F) MEFs from WT and SORLA KO mice were treated with induction medium, and expression of the indicated proteins was tested by Western blot analyses after $t = 5$ min. (E) Exemplary immunoblots of treated MEFs with induction cocktail. (F) Results of densitometric scanning of replicate blots ($n = 17$ – 36 independent experiments). Protein levels are given as relative to WT levels (set to 100%). Data are shown as mean \pm SEM. Statistical significance was evaluated using two-sided Student's t test. *, $P < 0.05$; **, $P < 0.01$; ***, $P < 0.001$. A normal distribution of data was assumed in D and F, but this was not formally tested. Numbers to the right of the blots are in kilodaltons.

increase in the levels of pIR, pAKT, or pERK was seen in Sca1^+ precursors from juvenile scWAT WT as compared with KO mice (Fig. 8, C and D, unstimulated or stimulated). The relevance of this tissue type-specific action of SORLA for adipogenesis was

substantiated by comparative expression analysis of adipocyte markers perilipin-1, adiponectin (*Adipoq*), and PPAR γ (*Pparg*). After 1 wk of differentiation, expression of these markers was significantly lower in Sca1^+ cell preparations from KO as

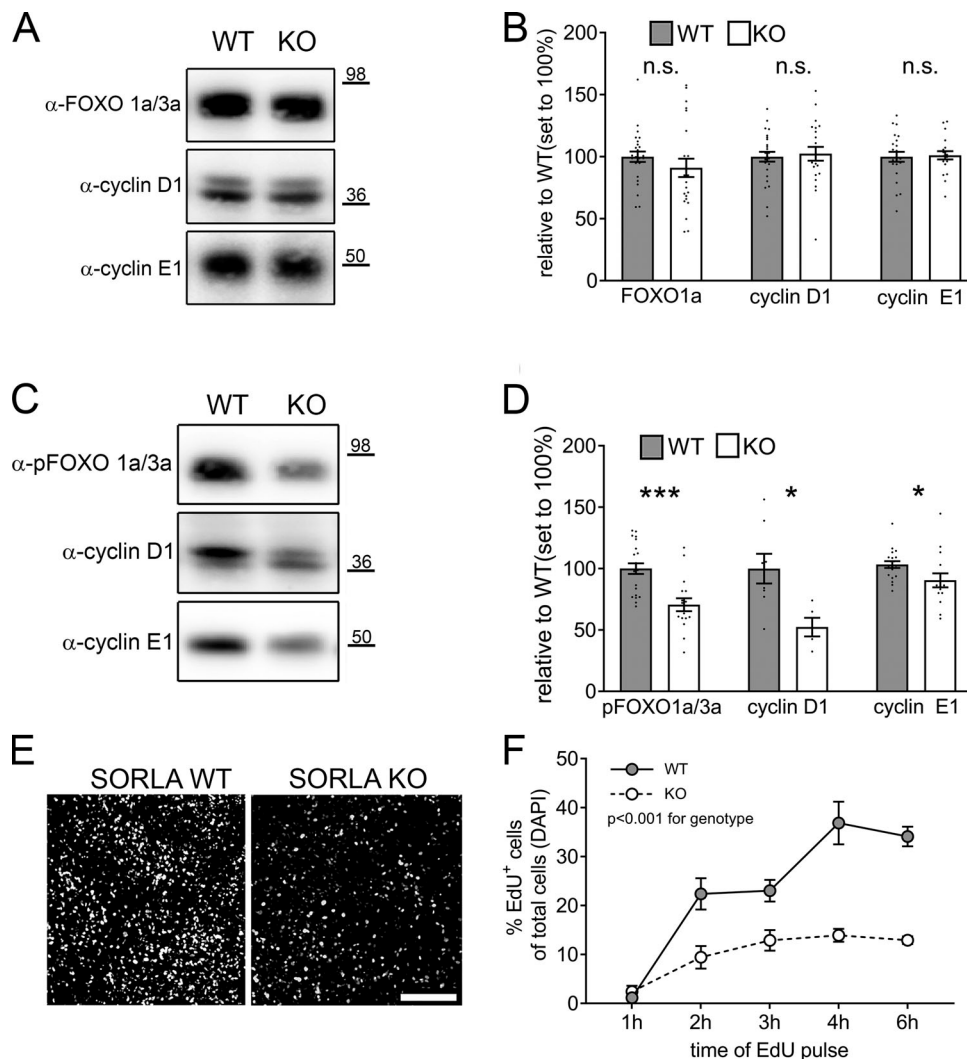


Figure 6. SORLA promotes insulin-induced mitotic expansion of adipocytes progenitors from MEFs. (A–D) MEFs from WT and SORLA KO mice were treated with induction medium and the amount of the indicated proteins in the cell extracts was determined by Western blotting at $t = 0$ min (A and B) and $t = 10$ min (C and D). (A and C) Representative Western blots. Numbers to the right of the blots are in kilodaltons. (B and D) Results of densitometric scanning of replicate blots ($n = 13$ – 26 independent experiments). Data are mean \pm SEM. Statistical significance of data was determined using two-sided Student's t test. *, $P < 0.05$; ***, $P < 0.001$. (E and F) MEFs from WT and SORLA KO mice were treated with induction medium for 18 h, followed by pulse-labeling with 10 μM EdU for the indicated times. Thereafter, the amount of EdU $^+$ cells in both genotypes was determined by immunocytochemistry. Representative images of EdU $^+$ cells in WT and SORLA KO MEFs after 3 h of EdU pulse are shown in E. (F) The total number of EdU $^+$ cells (as percentage of total number of DAPI $^+$ cells) scored over pulse-labeling time. Scale bar in E: 250 μm . Data in F are the mean \pm SEM from 7–10 individual experiments with 11,000–17,000 cells evaluated for each time point per genotype (two-way ANOVA for genotype, $P < 0.001$). A normal distribution of data was assumed in B, D, and F, but this was not formally tested.

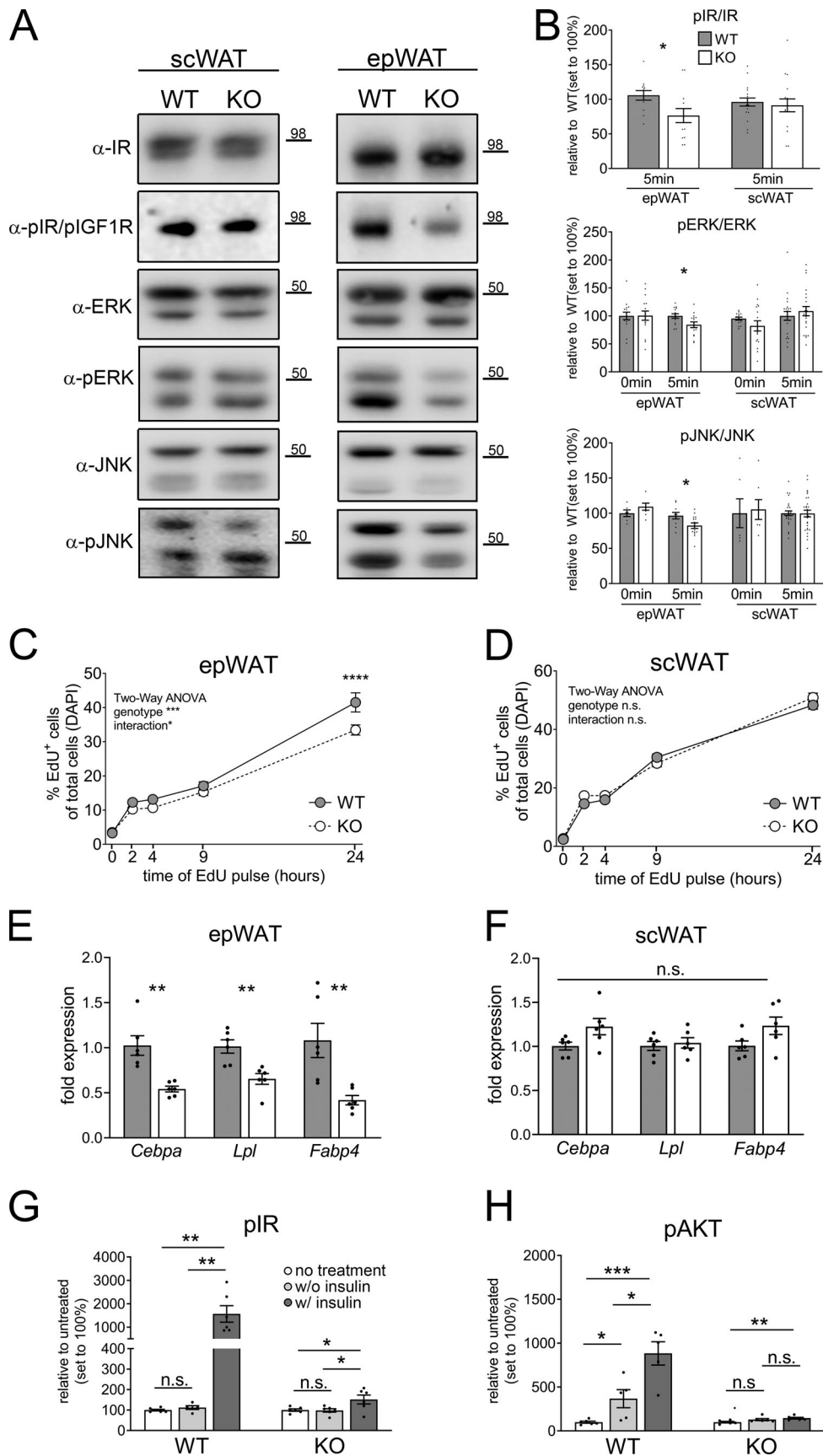


Figure 7. **SORLA promotes insulin-induced mitotic expansion of adipocyte precursors from ep but not scWAT.** (A and B) The SVFs from epWAT and scWAT of WT and KO mice were treated with induction medium and the amount of the indicated proteins in the cell extracts determined by Western blotting at

t = 5 min. **(A)** Representative Western blots. Numbers to the right of the blots are in kilodaltons. **(B)** The result of densitometric scanning of replicate blots (three to five independent experiments; $n = 8-22$). Data are the mean \pm SEM. Statistical significance of data was determined using two-sided Student's *t* test. *, $P < 0.05$. **(C and D)** SVFs from epWAT (C) and scWAT (D) of WT and KO mice were treated with induction medium for 18 h, followed by pulse-labeling with 10 μ M EdU for the indicated times. Thereafter, the amounts of EdU⁺ cells in both genotypes were determined by immunocytochemistry. Panels show the total number of EdU⁺ cells as percentage of total number of DAPI⁺ cells. Data are the mean \pm SEM from 19–24 independent experiments for each time point and genotype. Two-way ANOVA and Sidak's multiple comparisons test; *, $P < 0.05$; ***, $P < 0.001$; ****, $P < 0.0001$. **(E and F)** The SVFs from epWAT (E) and scWAT (F) of WT and KO mice were treated with induction medium and differentiated for 7 d. The amount of the indicated mature adipocyte marker proteins was determined using qPCR. Data are the mean \pm SEM ($n = 6$). Statistical significance of data was determined using two-sided Student's *t* test. **, $P < 0.01$. **(G and H)** Replicate cell layers of the SVFs from epWAT of WT and SORLA KO mice were either not treated or treated with induction medium containing (w/) or lacking (w/o) insulin. The response of the cells was measured at t = 5 min by determining the amount of phosphorylated forms of the IR (pIR; G) and AKT (pAKT; H) in the cell extracts using Western blotting. Data are the mean \pm SEM ($n = 6$) with protein levels of nontreated cells set to 100%. The statistical significance of data was determined using two-sided Student's *t* test. *, $P < 0.05$; **, $P < 0.01$; ***, $P < 0.001$. A normal distribution of data was assumed in B–D, G, and H, but this was not formally tested.

compared with WT epWAT (Fig. 8, E and F). No impact of receptor deficiency on adipocyte marker expression was observed in Sca1⁺ cells from scWAT of WT or KO animals (Fig. 8, E and G).

To document that the level of SORLA activity is a molecular determinant of the ability of adipocyte precursors to undergo mitotic expansion in response to insulin, we made use of a mouse strain carrying a Cre-inducible SORLA transgene inserted in the endogenous ROSA26 gene locus (Caglayan et al., 2014; Schmidt et al., 2016). To achieve SORLA overexpression in adipocyte precursors, we isolated the SVF from scWAT of juvenile WT mice and treated the cells with a recombinant cell-permeant version of Cre recombinase fused with the protein translocation peptide from HIV-TAT (TAT, trans-activator of transcription) and a nuclear localization sequence (Peitz et al., 2002). Cre-induced activation of the transgene strongly increased levels of SORLA in scWAT cells compared with untreated cells as shown by immunocytochemistry (Fig. 9 A) and Western blotting (Fig. 9 B). Increasing the already high levels of SORLA in the SVF from epWAT did not further raise the high proliferative capacity of these cells in response to insulin (Fig. 9 C). However, raising SORLA levels in scWAT cell preparations significantly enhanced their proliferative capacity when compared with nontreated controls (Fig. 9 C).

Taken together, our data identified SORLA as a molecular factor defining the unique proliferative property of the juvenile epWAT in response to diet. High levels of SORLA expression in adipocyte progenitors of the juvenile epWAT sensitize these cells to nutritional stimuli provided through insulin, promoting expansion of the vis precursor cell pool during overfeeding. By contrast, SORLA activity is relatively low in scWAT progenitors, blunting their response to insulin and preventing diet-induced progenitor pool propagation.

Discussion

Early studies in humans have demonstrated the different biological properties of visWAT versus scWAT, defining their distinct cardiometabolic risk profiles. Distinctions with particular relevance are timing and conditions that trigger expansion of these fat depots from a resident pool of early adipocyte progenitors. While expansion of scWAT mainly proceeds prenatally, visWAT expansion occurs in two periods in the early postnatal and the subsequent adolescent phase of life (Hirsch and Han, 1969; Holtrup et al., 2017; Kim et al., 2014; Tang et al., 2008;

Wang et al., 2013). Also, dietary surplus causes hyperplastic expansion of vis fat, whereas sc fat appears resistant to dietary stress (Jeffery et al., 2015; Kim et al., 2014; Kulenkampff and Wolfrum, 2019).

Our data recapitulate the enhanced precursor cell proliferation in juvenile murine epWAT compared with scWAT in vivo (Fig. 2 C) and in vitro (Fig. 7), and the susceptibility of this process to dietary stress (Fig. 2, D–F). Importantly, we uncovered that this age- and depot-specific effect of the diet on precursor cell proliferation is dependent on SORLA as loss of this receptor reduces the prominent expansion of precursor cell numbers in juvenile epWAT in response to overfeeding (Fig. 2, E and F). SORLA-dependent precursor cell proliferation coincides with the generation of mature adipocyte in MEFs (Fig. 5, A and B), as well as in SVF (Fig. 7, E and F) and Sca1⁺ precursor cell preparations (Fig. 8, E–G). Although not shown directly, the SORLA-dependent increase in precursor cell proliferation seen in the epWAT of WT mice in vivo is likely to also translate into larger numbers of mature adipocytes being produced. This conclusion is based on work from others documenting a direct correlation between precursor cell proliferation and generation of mature adipocytes (Berry and Rodeheffer, 2013; Wang et al., 2013).

In earlier studies, inherent mechanisms, such as distinct identities of adipocyte precursors (Gesta et al., 2006; Macotela et al., 2012), but also differences in the microenvironment (Jeffery et al., 2016; Kulenkampff and Wolfrum, 2019), have been held responsible for the unique adipogenic properties of visWAT as compared with scWAT. Our data now identify SORLA as a molecular factor that defines the ability of epWAT precursors to proliferate in response to dietary input, an activity most prevalent in the juvenile organism (Fig. 2, D–F). Because *Sorl1* transcript levels correlate with the extent of cell proliferation in juvenile versus adult fat tissues (Fig. 3 B) and because precursor cell proliferation in scWAT can be promoted by increasing its expression levels (Fig. 9), the activity level of SORLA appears to be a crucial determinant of the depot-specific proliferative properties of adipocyte precursors. Our hypothesis is supported by scRNAseq data documenting robust expression of *SORL1* in adipocyte precursors in human visWAT, but not scWAT (Fig. 1 H).

Several signaling factors have been implicated in promoting proliferation of adipocyte precursors. For example, transcription factor forkhead box C2 protein enhances cyclin E expression and increases proliferation in vis preadipocyte, likely acting

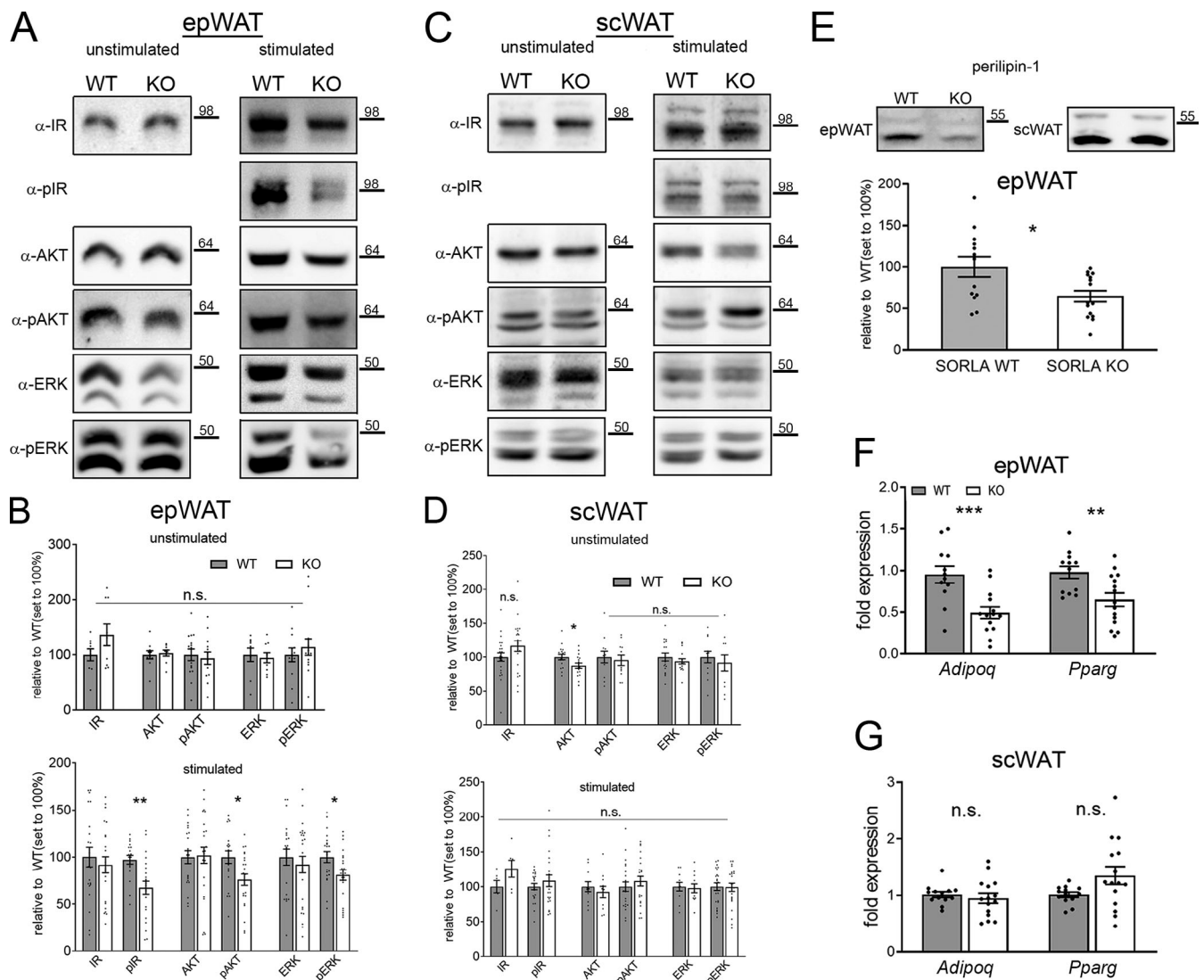


Figure 8. SORLA promotes adipogenesis of Sca1⁺ precursor cells from ep but not scWAT. (A–D) Lin-CD34⁺CD29⁺Sca1⁺ precursor cells sorted from epWAT (A and B) and scWAT (C and D) of WT and KO mice were treated with induction medium. The amount of the indicated proteins in the cell extracts was determined by Western blot analysis after 5 min treatment (stimulated) or no treatment (unstimulated). **(A and C)** Representative Western blots. **(B and D)** The result of densitometric scanning of replicate blots (three independent experiments; $n = 12–26$). Data are the mean \pm SEM. Statistical significance of data was determined using two-sided Student's t test. *, $P < 0.05$; **, $P < 0.01$. **(E–G)** Lin-CD34⁺CD29⁺Sca1⁺ precursor cells from epWAT and scWAT of WT and KO mice were treated with complete induction medium for 7 d. Thereafter, the amount of the indicated mature adipocyte marker proteins was determined by Western blot analysis (E) or quantitative RT-PCR (F and G). Data are the mean \pm SEM ($n = 12–15$). Statistical significance of data was determined using two-sided Student's t test. *, $P < 0.05$; **, $P < 0.01$; ***, $P < 0.001$. A normal distribution of data was assumed in B and D–F, but this was not formally tested. Numbers to the right of the blots are in kilodaltons.

downstream of mammalian target of rapamycin (Gan et al., 2015). Also, estrogen receptors (Zhang et al., 2016b) and inhibitor of metalloprotease-1 (TIMP-1; Zhang et al., 2016a) have been shown to control adipose-derived stem cell proliferation. Whether these mechanisms act differently on precursors from vis and scWAT has not been explored so far. We now document that SORLA promotes the mitotic expansion of precursor cells in vitro and that this mechanism is operable in precursors from epWAT but not scWAT (Fig. 7, C and D), providing a molecular explanation for the inherent proliferative properties of both tissues. By contrast, the receptor activity seems dispensable for subsequent steps in adipocyte maturation as shown in MEFs

(Fig. S3, A–C). The latter findings also argue against a non-specific effect of SORLA deficiency on cell viability, although such an effect cannot be fully excluded.

We also document that the signal(s) that act through SORLA to promote progenitor pool expansion in vivo derive from a nutritional input (Fig. 2, D–F). We cannot deduce the identity of the responsible signaling molecule with absolute certainty, but our findings strongly argue for insulin as shown by the blunted response of SORLA-deficient cells to this hormone in terms of phosphorylation of the IR and AKT (Fig. 7, G and H). In support of our model, insulin conveys signals from nutritional input to adipose tissue (Blüher et al., 2002; Boucher et al., 2010), and

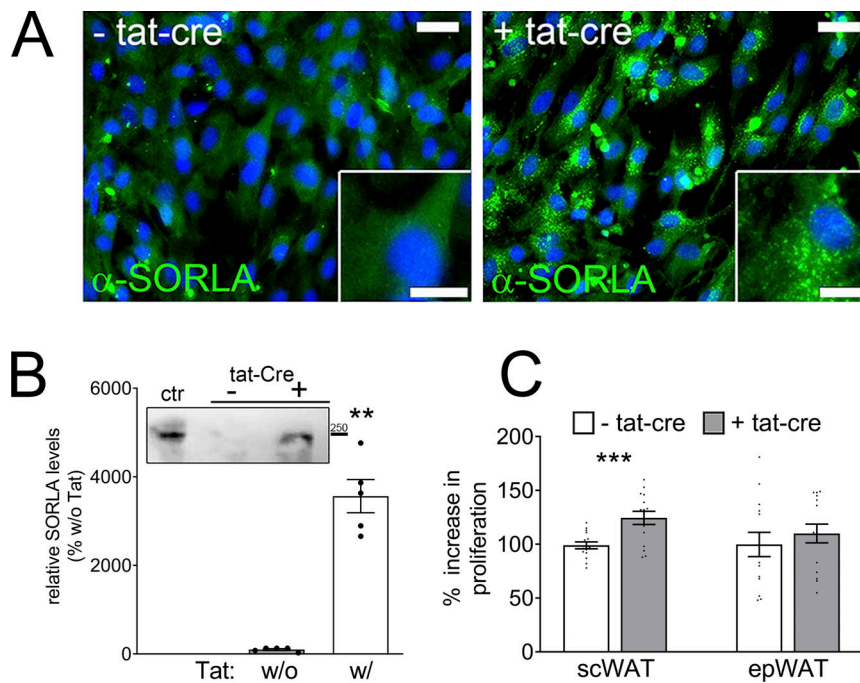


Figure 9. SORLA overexpression increases the insulin-dependent proliferative capacity of scWAT. (A and B) The SVF was isolated from epWAT and scWAT of juvenile mice carrying a Cre-inducible SORLA transgene in the endogenous *Rosa26* gene locus (Caglayan et al., 2014; Schmidt et al., 2016). To induce SORLA overexpression, replicate cell layers were treated for 3 h with 6.6 μ M of purified Cre recombinase consisting of a N-terminal 6x His tag, a TAT peptide, and an NLS sequence (HTNCre; ExcCellgen). SORLA overexpression after 3 d of Cre induction in scWAT adipocyte precursor cells (+ tat-cre) as compared with nontreated cells (- tat-cre) is exemplified by immunocytochemistry (A) and Western blot analysis (B). The insets in A depict higher magnification images of SORLA expression (green) in the respective cell cultures. Western blot analysis in B documents increased levels of SORLA in Cre-treated (w/) compared with nontreated (w/o) SVF cells of scWAT. As a positive control, the SVFs purified from the scWAT of SORLA transgenic mice stably expressing Cre recombinase were tested as well (ctr). Significance of data was determined using the two-sided Mann-Whitney test; data are the mean \pm SEM ($n = 5$); **, $P < 0.01$. Scale bar in A: 50 μ m (inset: 25 μ m). The number to the right of the blot is in kilodaltons. **(C)** SVF cells from scWAT and epWAT nontreated or treated with HTNCre were pulse-labeled with EdU for 6 h. The number of EdU⁺ cells was scored by immunocytochemistry and expressed as the percent increase in cell count as compared with cultures without induction of SORLA overexpression (no induction set to 100%). Induction of SORLA overexpression results in a significantly higher increase in proliferation as compared with the noninduced condition in scWAT, but not in epWAT. Data are the mean \pm SEM from $n = 5$ independent experiments per tissue and condition (three images per experiment). Significance of data was determined using two-sided Student's *t* test; ***, $P < 0.001$. Data distribution was assumed to be normal, but this was not formally tested.

short-term HFD exposure induces AKT phosphorylation, a prominent hub of insulin signaling in vis adipocyte precursors (Jeffery et al., 2015). Also, stimulation of the insulin pathway is a major mechanism whereby progenitors are committed into adipogenesis (Green and Kehinde, 1975; Tang et al., 2008), and its function in promoting cell proliferation in adipose tissues was shown in diabetic rats after insulin infusion (Géloën et al., 1989). Conceptually, SORLA deficiency may impact adipogenesis by other defects more fundamental than insulin signaling. Such a hypothesis may be tested by comparing the residual adipogenic potential of WT and KO precursors in response to an induction medium lacking insulin. However, in our hands, even WT cells failed to respond to such conditions with induction of adipogenic gene expression and lipid accumulation (data not shown), in line with data reported by others before (Guller et al., 1988; Négrelet al., 1978).

Foremost, a proposed cell autonomous effect of SORLA on insulin signaling in adipocyte precursor cells is supported by its established function as retrieval factor for the IR. Specifically, SORLA promotes cell surface recycling of internalized IR molecules, thereby facilitating insulin signal reception in target cells

(Schmidt et al., 2016). In line with a role for SORLA in promoting insulin signaling, loss of the receptor blunts activation of MAPK pathway components ERK and JNK as well as the PI3K/AKT pathway in adipocyte precursors (Figs. 5, E and F; Fig. 7, A and B; and Fig. 8, A and B). These pathways act downstream of insulin in stimulating adipogenesis (Accili and Taylor, 1991; Tomiyama et al., 1995; Bost et al., 2005; Tang et al., 2005; Park et al., 2014). According to our model, high levels of SORLA specific to juvenile epWAT precursors sensitize these cells to insulin derived from nutritional signals. Consequently, low receptor levels, as in scWAT or in adult epWAT, render these cells relatively insensitive to insulin-derived mitogenic stimuli. While our data provide evidence for the importance of a cell-autonomous action of SORLA in control of precursor cell proliferation, they do not rule out non-cell-autonomous mechanisms whereby the epWAT contributes to a pro-mitogenic milieu. This assumption is supported by our transplantation experiments where precursors in the KO in WT condition trended with intermediate levels of proliferation between KO in KO and WT in WT, although this trend did not reach statistical significance (Fig. 4 C). Conceptually, such non-cell-autonomous mechanisms may be dependent

(i.e., ectodomain shedding) or independent of SORLA expression in this tissue.

In humans, *SORL1* has been specifically associated with the longitudinal risk of obesity (Smith et al., 2010). Prenatal or juvenile mechanisms implicated in the longitudinal risk of obesity in rodent models include maternal overfeeding during pregnancy or weaning (Guberman et al., 2013; Kayser et al., 2015). Juvenile overfeeding may impact adult risk of obesity for several reasons, potentially including the determination of the adipocyte precursor pool size. In this respect, SORLA-dependent expansion of the adipocyte precursor pool in juvenile epWAT in response to overfeeding may pose a unique mechanism whereby the juvenile metabolism impacts on adult energy homeostasis. Whether increased numbers of precursors are beneficial by increasing the number of mature adipocytes in obesity (Arner et al., 2010; Kim et al., 2014) or detrimental by contributing to diet-induced hyperplasia of vis fat (Muir et al., 2016; Spalding et al., 2008) remains a matter of debate. Irrespective of whether an increased precursor cell pool is ultimately good or bad for adult health, it is tempting to speculate that genetically determined *SORL1* levels specific to visWAT precursors define the response of an individual to dietary input at the juvenile age, a process that impacts the progenitor pool size in visWAT and, ultimately, adult metabolism.

Materials and methods

Quantification of protein levels

Relative protein levels in cells and tissue were determined by densitometric scanning of replicate Western blots using ImageJ software. Antibodies against SORLA were generated in house. The following antibodies were purchased from Cell Signaling: pIR/pIGF1R (#3024), IR (#3025), IGF1R (#9750), pIGF1R (#4568), adiponectin (#2789), perilipin (#9349), GLUT4 (#2213), AKT (#4691), and pAKT-Thr (#2965), ERK (#9102), pERK (#4695), MKK4 (#3346), pMKK4 (#4514), JNK (#9258), pJNK (#9251), FOXO1a (#2880), pFOXO1a/3a (#9464), cyclin D1 (#2978), cyclin E1 (#20808), calnexin (#2433), and β -tubulin (#5568).

Patient studies

For quantitative PCR (qPCR) analysis of *SORL1* transcripts, paired samples of vis or sc whole adipose tissue were obtained from 362 individuals (246 women and 116 men). The age ranged from 19 to 93 yr (Klötting et al., 2010). BMI was calculated by weight (kg) divided by square of height (m). All adipose tissue samples were collected during open or laparoscopic abdominal surgery, immediately frozen in liquid nitrogen, and stored at -80°C . The study on human adipose specimens was approved by the Ethics Committee of the University of Leipzig (approval no. 159-12-21052012) and performed in accordance with the Declaration of Helsinki. All subjects gave written informed consent before taking part in this study.

Re-analysis of deposited scRNAseq data from human stromal vascular WAT

Normalized scRNAseq data reported by Vijay et al. (2020) of the SVF of human visWAT and scWAT were downloaded from GEO

(accession no. GSE136230). In brief, data were available from 14,371 cells derived from nine nondiabetic but obese middle-aged individuals (male/female, 2/7; age, mean \pm SD, 43.3 \pm 11.4; BMI, mean \pm SD, 43.3 \pm 11.4). Based on expression characteristics of reported cell type markers (Vijay et al., 2020), individual cells were annotated to the indicated subsets of cell types using hierarchical clustering (Euclidian, Ward). *SORL1* expressing cells were defined as cells with *SORL1* transcripts per million \neq 0.

Animal experimentation

Mice with targeted disruption of *Sorl1* (referred to as SORLA KO) have been described before (Andersen et al., 2005). All studies were performed comparing male SORLA KO with SORLA WT control animals on an inbred C57BL/6-J background. The animals were kept on a standard mouse chow (4.5% crude fat, 39% carbohydrates; Sniff Deutschland; V1124-3) or on an HFD (35% crude fat, 10% carbohydrate; Sniff Deutschland; E15741-34). All animal experimentation was conducted following approval by local authorities of the Federal State of Berlin (X9007/17, G0156/19).

Cell transplantation experiments

The SVF was isolated from the epWAT of juvenile donor mice, sorted for adipocyte precursors, and transplanted into the scWAT pad of adult recipients via Matrigel (Corning; #354234) injections. Four animals were used per Matrigel pad. Subsequently, recipients received EdU (ab146186) at 200 $\mu\text{g}/\text{ml}$ for 14 d in drinking water to label proliferative cells while being on an HFD for 5 wk (35% fat, 23.9% protein, 4.9% fibers, 5% ashes; Provimi Kliba SA) to induce proliferation in the transplanted tissue pads. Thereafter, the Matrigel pads were carefully excised and fixed overnight in 4% paraformaldehyde. The pads were washed in water and processed with the STP120 Spin Tissue Processor (Thermo Fisher Scientific), followed by paraffin embedding. Histological sections of transplanted tissue pads were immunostained for EdU (SULFO-Cy3-Azide method) and DAPI. The numbers of EdU⁺ cells and total cell count (DAPI) in transplanted tissue pads were determined using ImageJ software.

Flow-cytometric analysis of endogenous adipocyte precursor cells

For proliferation analysis, mice were treated with BrdU (800 $\mu\text{g}/\text{ml}$) in drinking water for 3 d before sacrifice. SVFs were obtained from sc and visWAT for flow-cytometric analysis as follows. Tissues were excised, minced, and digested in collagenase/Hepes solution for 75 min at 37°C . HBSS (Sigma-Aldrich; H8264) with 3% BSA was added to the homogenates and centrifuged for 3 min at $300 \times g$. Floating adipocytes were removed and the SVFs homogenized in HBSS/3% BSA, then centrifuged again, and the pellets were homogenized and filtered through a 40- μm mesh filter. For counting and sorting of adipocyte precursors, cells were stained for 60 min on ice in HBSS/3% BSA with the following antibodies: CD45 APC-eFluor 780 (eBioscience; 47-0451-82; 1:3,000), CD31 PE-Cy7 (eBioscience; 25-0311-82; 1:1,000), CD29 BV421 (Becton Dickinson; 564131; 1:100), CD34 Alexa Fluor 647 (BioLegend; 119314; 1:200), Scal brilliant violet (BioLegend; 108129; 1:200), and CD24 PE (BioLegend; 101808; 1:100). For

counting and sorting of other cell types in SVFs, cells were stained for 60 min on ice in HBSS/3% BSA with the following antibodies: CD11b FITC (Miltenyi Biotec; 130-113-234; 1:50), CD8 BV650 (BioLegend; 100741; 1:100), CD19 PE (BioLegend; 152408; 1:200), and CD4 APC (BioLegend; 100412; 1:100). Following antibody incubation, the cell preparations were washed with HBSS/3% BSA and filtered into a FACS tube.

For BrdU analysis, cells were stained as above and then fixed and permeabilized with Phosflow lyse/fix (Becton Dickinson; 558049) and Perm Buffer III (Becton Dickinson; 558050) according to the manufacturer's recommendations. Cells were treated with DNase (Invitrogen; 18047019; final concentration, 50–375 U) in PBS with 6 mM MgCl₂ and 1 mM CaCl₂ for 2 h in a 37°C water bath. Then the cells were washed in HBSS/3% BSA and incubated with anti-BrdU antibody (Alexa Fluor 488; BioLegend; 364106; 1:100) overnight at 4°C. Finally, the cells were washed and analyzed on a BD FACS Aria 2 analyzer. Data analysis was performed using BD FACS Diva Software and FlowJo V10.

Induction of SORLA expression by Cre recombinase

The SVF was cultured from ep and scWAT of mice carrying a Cre-inducible SORLA expression construct inserted into the endogenous *Rosa26* gene locus (Caglayan et al., 2014). To induce SORLA overexpression, replicate cell layers were treated with 6.6 μM of purified Cre recombinase protein consisting of an N-terminal 6x His tag, a TAT peptide, and an NLS sequence (HTNCre) and with 100 μM chloroquine for 3 h (Excellgen; EG-1001). Cells were washed and further incubated until confluency. After 3 d, the adipocyte differentiation cocktail was applied to the confluent cell layers and EdU treatment started 18 h later for 6 h before fixing the cells and performing immunodetection of SORLA, EdU, and DAPI staining. Quantification of EdU⁺ and DAPI⁺ cells was done using ImageJ software.

In vivo analysis of adipocyte progenitor cell proliferation in mice

Mice were treated with 200 μg/ml EdU in drinking water for 3 or 7 d. Thereafter, adipose tissues were harvested and fixed in 4% PFA/PBS for 8–16 h at 4°C. After 1 h of washing in PBS, the tissues were dehydrated, embedded in paraffin, and cut in 10-μm sections. For EdU detection, sections were incubated for 5 min in 100 mM Tris, permeabilized in PBS with 0.5% Triton X-100 for 30 min, and washed three times for 5 min in PBS. Then the tissues were incubated with detection solution (2 mM CuSO₄, 20 mg/ml ascorbic acid, and 8 μM SULFO-Cy3-Azide [Lumiprobe; #81330] in PBS) for 30 min, followed by three washes for 5 min in PBS. Finally, the sections were incubated for 5 min in DAPI/PBS, washed again in PBS, and mounted with DAKO Fluorescence Mounting Medium. The number of EdU⁺ cells and the total cell count (DAPI) were determined from three sections per animal using ImageJ software.

Primary and MEF cell-derived adipocyte cultures

Primary adipocytes were differentiated from preadipocytes or Lin⁻CD34⁺CD29⁺Sca1⁺-sorted cells isolated from WAT or from MEFs. In brief, WAT was removed, minced, and digested with collagenase/Hepes solution for 45–60 min at 37°C. Cells were

incubated with red blood cell lysis buffer (155 mM NH₄Cl, 10 mM KHCO₃, and 0.1 mM EDTA) for 5 min and filtered through a 20-μm mesh filter to obtain the SVF. To generate MEFs, embryonic day 14.5 mouse embryos were dissected and trypsinized for 30 min at 37°C. After centrifugation (1,000 ×g, 10 min), the cell pellets were resuspended in DMEM supplemented with 10% FBS and plated on culture dishes.

For adipocyte differentiation, MEFs or stromal vascular cells including preadipocytes were cultured to confluency. 3 d later, the medium was replaced with induction medium containing DMEM supplemented with 5% FBS, 17 nM insulin (Sigma-Aldrich; I6634), 0.1 μM dexamethasone (Sigma-Aldrich; D4902), 250 μM 3-isobutyl-1-methylxanthine (Sigma-Aldrich; I5879), 1 μM rosiglitazone (Sigma-Aldrich; R2408), and 60 μM indomethacin (Sigma-Aldrich; I7378; only for preadipocyte preparation). After the indicated time points, cells were harvested and snap-frozen in liquid nitrogen for further analysis of protein and mRNA levels. For complete adipocyte differentiation, 2 d after induction, the cells were grown in DMEM/10% FBS with insulin for another 2 d. After 7–14 d of culture in normal growth medium (DMEM/10% FBS), the adipocytes were lipid-filled and ready for Western blot analysis, qPCR, or Oil Red O staining.

Oil Red O staining

Differentiated cells were rinsed three times with HBSS (Sigma-Aldrich; H1387) and fixed in cold Baker's Formalin (3.7% formaldehyde and 1% CaCl₂ in distilled water) for 30 min at 4°C. Thereafter, the fixation solution was removed, and filtered 60% Oil Red O solution (Sigma-Aldrich; O0625) was applied to the cells for 10 min at RT. Afterward, the staining solution was removed and the cell preparation cleaned in running tap water (3–5 min). Finally, the cell layers were recovered and the Oil Red O staining intensity determined using a standard Photometer at OD 500 nm.

Proliferation analyses in MEF and adipocyte precursor cells

MEF and adipocyte precursor cells from SVF were grown in 48-well plates until 2 d after confluency. Cells were treated with induction medium to start adipocyte differentiation. After 18 h, EdU was added to the differentiation medium at a final concentration of 10 μM for the indicated time points. Cells were then washed in PBS/3% BSA, fixed in 3.7% formaldehyde/PBS for 15 min, washed again, and permeabilized in 0.5% Triton X-100/PBS for 20 min at RT. The Click-iT EdU Alexa Fluor 488 Imaging Kit (Invitrogen; C10337) was used to detect EdU incorporation into the genomic DNA according to the manufacturer's instructions.

qPCR analysis of MEF and adipocyte precursor cells

For transcriptomics analysis, RNA from MEFs or SVF at various stages of adipocyte differentiation were extracted using the RNeasy Lipid Tissue Mini Kit (QIAGEN). The quantity and integrity of the RNA preparation were determined using a NanoVue plus Spectrophotometer (GE Healthcare). 1 μg of total RNA was reverse-transcribed using standard reagents (Life Technologies) and cDNA processed for TaqMan probe-based qPCR using the QuantStudio 6 Flex Real-Time PCR System

(Life Technologies). Expression of *Cebpd* (Mm00786711_s1), *Cebpb* (Mm00843434_s1), *Cebpα* (Mm00514283_s1), *Pparg* (Mm00440940_m1), *Lpl* (Mm01345521_m1), *Fabp4* (Mm00445878_m1), and adiponectin (Mm00456425_m1) was calculated by the standard curve method and normalized to the expression of 18S ribosomal RNA (rRNA; 4352930E) or *Gapdh* (Mm99999915_g1; Life Technologies) as internal controls.

To determine *Sorl1* (Mm01169526_m1) transcript levels in adipocyte precursor cells, the SVF was isolated from ep and sc adipose tissues and FACS-sorted for Lin⁻CD34⁺CD29⁺Sca1⁺ cells, followed by RNA isolation.

Microscope image acquisition

The microscopic images were acquired using a Leica Microsystems CMS GmbH apparatus (model DMi8) with 10×, 40×, or 63× objectives and a Leica K5 or DMC2900 camera at RT. Image analysis was performed using Leica Application Suite X (LAS X version 3.7.4.23463) and ImageJ.

Statistics

Statistical analyses were performed using GraphPad Prism 8 Software. Data are presented as mean ± SEM. For comparing two groups, unpaired two-sided Student's *t* test, unpaired two-sided Mann–Whitney test, or paired Wilcoxon test was used. For experiments with more than two groups, unmatched two-sided one-way ANOVA followed by Tukey's multiple comparisons test was used. For experiments with more than two parameters, unmatched two-sided two-way ANOVA with Sidak's multiple comparison test was applied. For association studies, linear regression analysis with Pearson correlation coefficient was used. Data distribution for the parametric tests was assumed to be normal, but this was not formally tested.

Online supplemental material

Fig. S1 shows the multicolor FACS strategy and exemplary scatter plots of cells from the murine SVF of WAT during FACS sorting. Proliferating adipocyte progenitors are identified using the markers CD45⁻CD31⁻CD29⁺CD34⁺Sca1⁺BrdU⁺. **Fig. S2** shows exemplary scatter plots and the percent distribution of different cell types after FACS sorting of the murine SVF of WAT. **Fig. S3** shows the adipogenic differentiation potential of MEFs from SORLA WT and KO mice. Markers for early differentiation are unchanged while markers for mature adipocytes are reduced in KO animals.

Acknowledgments

We are indebted to T. Pasternack, R. Vogel, M. Ströhmman, and M. Kahlow for expert technical assistance.

Studies were funded in part by the European Research Council (BeyOND no. 335692), the Helmholtz Association (iCEMED HA-314, AMPPro ZT-0026), and the Novo Nordisk Fonden.

The authors declare no competing financial interests.

Author contributions: V. Schmidt designed and performed all experiments; C. Horváth and H. Dong performed the transplantation experiment; P. Qvist analyzed the scRNAseq data; V.

Schmidt, C. Horváth, C. Wolfrum, and T.E. Willnow evaluated data. M. Blüher provided essential human biospecimens. T.E. Willnow wrote the manuscript with input from all authors.

Submitted: 10 June 2020

Revised: 19 June 2021

Accepted: 8 September 2021

References

- Accili, D., and S.I. Taylor. 1991. Targeted inactivation of the insulin receptor gene in mouse 3T3-L1 fibroblasts via homologous recombination. *Proc. Natl. Acad. Sci. USA.* 88(11):4708–4712. <https://doi.org/10.1073/pnas.88.11.4708>
- Andersen, O.M., J. Reiche, V. Schmidt, M. Gotthardt, R. Spoelgen, J. Behlke, C.A. von Arnim, T. Breiderhoff, P. Jansen, X. Wu, et al. 2005. Neuronal sorting protein-related receptor sorLA/LR11 regulates processing of the amyloid precursor protein. *Proc. Natl. Acad. Sci. USA.* 102:13461–13466. <https://doi.org/10.1073/pnas.0503689102>
- Arner, E., P.O. Westermark, K.L. Spalding, T. Britton, M. Rydén, J. Frisén, S. Bernard, and P. Arner. 2010. Adipocyte turnover: relevance to human adipose tissue morphology. *Diabetes.* 59:105–109. <https://doi.org/10.2337/db09-0942>
- Baldin, V., J. Lukas, M.J. Marcote, M. Pagano, and G. Draetta. 1993. Cyclin D1 is a nuclear protein required for cell cycle progression in G1. *Genes Dev.* 7: 812–821. <https://doi.org/10.1101/gad.7.5.812>
- Berry, R., and M.S. Rodeheffer. 2013. Characterization of the adipocyte cellular lineage in vivo. *Nat. Cell Biol.* 15:302–308. <https://doi.org/10.1038/ncb2696>
- Blüher, M., M.D. Michael, O.D. Peroni, K. Ueki, N. Carter, B.B. Kahn, and C.R. Kahn. 2002. Adipose tissue selective insulin receptor knockout protects against obesity and obesity-related glucose intolerance. *Dev. Cell.* 3: 25–38. [https://doi.org/10.1016/S1534-5807\(02\)00199-5](https://doi.org/10.1016/S1534-5807(02)00199-5)
- Bost, F., M. Aouadi, L. Caron, P. Even, N. Belmonte, M. Prot, C. Dani, P. Hofman, G. Pages, J. Pouyssegur, et al. 2005. The Extracellular Signal-Regulated Kinase Isoform ERK1 Is Specifically Required for In Vitro and In Vivo Adipogenesis. *Diabetes.* 54(2):402–411. <https://doi.org/10.2337/diabetes.54.2.402>
- Boucher, J., Y.H. Tseng, and C.R. Kahn. 2010. Insulin and insulin-like growth factor-1 receptors act as ligand-specific amplitude modulators of a common pathway regulating gene transcription. *J. Biol. Chem.* 285: 17235–17245. <https://doi.org/10.1074/jbc.M110.118620>
- Caglayan, S., S. Takagi-Niidome, F. Liao, A.S. Carlo, V. Schmidt, T. Burgert, Y. Kitago, E.M. Fuchtbauer, A. Fuchtbauer, D.M. Holtzman, et al. 2014. Lysosomal sorting of amyloid-β by the SORLA receptor is impaired by a familial Alzheimer's disease mutation. *Sci. Transl. Med.* 6:223ra20. <https://doi.org/10.1126/scitranslmed.3007747>
- Cinti, S. 2012. The adipose organ at a glance. *Dis. Model. Mech.* 5:588–594. <https://doi.org/10.1242/dmm.009662>
- Di Angelantonio, E., ShN. Bhupathiraju, D. Wormser, P. Gao, S. Kaptoge, A. Berrington de Gonzalez, B.J. Cairns, R. Huxley, ChL. Jackson, G. Joshy, et al. Global BMI Mortality Collaboration. 2016. Body-mass index and all-cause mortality: individual-participant-data meta-analysis of 239 prospective studies in four continents. *Lancet.* 388:776–786. [https://doi.org/10.1016/S0140-6736\(16\)30175-1](https://doi.org/10.1016/S0140-6736(16)30175-1)
- Eto, H., H. Suga, D. Matsumoto, K. Inoue, N. Aoi, H. Kato, J. Araki, and K. Yoshimura. 2009. Characterization of structure and cellular components of aspirated and excised adipose tissue. *Plast. Reconstr. Surg.* 124: 1087–1097. <https://doi.org/10.1097/PRS.0b013e3181b5a3f1>
- Gan, L., Z. Liu, W. Jin, Z. Zhou, and C. Sun. 2015. Foxc2 enhances proliferation and inhibits apoptosis through activating Akt/mTORC1 signaling pathway in mouse preadipocytes. *J. Lipid Res.* 56:1471–1480. <https://doi.org/10.1194/jlr.M057679>
- Géloën, A., A.J. Collet, G. Guay, and L.J. Bukowiecki. 1989. Insulin stimulates in vivo cell proliferation in white adipose tissue. *Am. J. Physiol.* 256: C190–C196. <https://doi.org/10.1152/ajpcell.1989.256.1.C190>
- Geserick, M., M. Vogel, R. Gausche, T. Lipek, U. Spielau, E. Keller, R. Pfäffle, W. Kiess, and A. Körner. 2018. Acceleration of BMI in Early Childhood and Risk of Sustained Obesity. *N. Engl. J. Med.* 379:1303–1312. <https://doi.org/10.1056/NEJMoa1803527>
- Gesta, S., M. Blüher, Y. Yamamoto, A.W. Norris, J. Berndt, S. Kralisch, J. Boucher, C. Lewis, and C.R. Kahn. 2006. Evidence for a role of

- developmental genes in the origin of obesity and body fat distribution. *Proc. Natl. Acad. Sci. USA.* 103:6676–6681. <https://doi.org/10.1073/pnas.0601752103>
- Green, H., and O. Kehinde. 1975. An established preadipose cell line and its differentiation in culture. II. Factors affecting the adipose conversion. *Cell.* 5:19–27. [https://doi.org/10.1016/0092-8674\(75\)90087-2](https://doi.org/10.1016/0092-8674(75)90087-2)
- Guberman, C., J.K. Jellyman, G. Han, M.G. Ross, and M. Desai. 2013. Maternal high-fat diet programs rat offspring hypertension and activates the adipose renin-angiotensin system. *Am. J. Obstet. Gynecol.* 209:262.e1–262.e8. <https://doi.org/10.1016/j.ajog.2013.05.023>
- Guller, S., R.E. Corin, D.C. Mynarcik, B.M. London, and M. Sonenberg. 1988. Role of insulin in growth hormone-stimulated 3T3 cell adipogenesis. *Endocrinology.* 122:2084–2089. <https://doi.org/10.1210/endo-122-5-2084>
- Hirsch, J., and P.W. Han. 1969. Cellularity of rat adipose tissue: effects of growth, starvation, and obesity. *J. Lipid Res.* 10:77–82. [https://doi.org/10.1016/S0022-2275\(20\)42651-3](https://doi.org/10.1016/S0022-2275(20)42651-3)
- Holtrup, B., C.D. Church, R. Berry, L. Colman, E. Jeffery, J. Bober, and M.S. Rodeheffer. 2017. Puberty is an important developmental period for the establishment of adipose tissue mass and metabolic homeostasis. *Adipocyte.* 6:224–233. <https://doi.org/10.1080/21623945.2017.1349042>
- Jeffery, E., C.D. Church, B. Holtrup, L. Colman, and M.S. Rodeheffer. 2015. Rapid depot-specific activation of adipocyte precursor cells at the onset of obesity. *Nat. Cell Biol.* 17:376–385. <https://doi.org/10.1038/ncb3122>
- Jeffery, E., A. Wing, B. Holtrup, Z. Sebo, J.L. Kaplan, R. Saavedra-Peña, C.D. Church, L. Colman, R. Berry, and M.S. Rodeheffer. 2016. The Adipose Tissue Microenvironment Regulates Depot-Specific Adipogenesis in Obesity. *Cell Metab.* 24:142–150. <https://doi.org/10.1016/j.cmet.2016.05.012>
- Kayser, B.D., M.I. Goran, and S.G. Bouret. 2015. Perinatal overnutrition exacerbates adipose tissue inflammation caused by high-fat feeding in C57BL/6j mice. *PLoS One.* 10:e0121954. <https://doi.org/10.1371/journal.pone.0121954>
- Kim, S.M., M. Lun, M. Wang, S.E. Senyo, C. Guillermier, P. Patwari, and M.L. Steinhauser. 2014. Loss of white adipose hyperplastic potential is associated with enhanced susceptibility to insulin resistance. *Cell Metab.* 20:1049–1058. <https://doi.org/10.1016/j.cmet.2014.10.010>
- Klötting, N., M. Fasshauer, A. Dietrich, P. Kovacs, M.R. Schön, M. Kern, M. Stumvoll, and M. Blüher. 2010. Insulin-sensitive obesity. *Am. J. Physiol. Endocrinol. Metab.* 299:E506–E515. <https://doi.org/10.1152/ajpendo.00586.2009>
- Kulenkampff, E., and C. Wolfrum. 2019. Proliferation of nutrition sensing preadipocytes upon short term HFD feeding. *Adipocyte.* 8:16–25. <https://doi.org/10.1080/21623945.2018.1521229>
- Liu, P., F. Kong, J. Wang, Q. Lu, H. Xu, T. Qi, and J. Meng. 2015. Involvement of IGF-1 and MEOX2 in PI3K/Akt1/2 and ERK1/2 pathways mediated proliferation and differentiation of perivascular adipocytes. *Exp. Cell Res.* 331:82–96. <https://doi.org/10.1016/j.yexcr.2014.09.011>
- Macotella, Y., B. Emanuelli, M.A. Mori, S. Gesta, T.J. Schulz, Y.H. Tseng, and C.R. Kahn. 2012. Intrinsic differences in adipocyte precursor cells from different white fat depots. *Diabetes.* 61:1691–1699. <https://doi.org/10.2337/db11-1753>
- Miao, Z., M. Alvarez, A. Ko, Y. Bhagat, E. Rahmani, B. Jew, S. Heinonen, L.L. Muñoz-Hernandez, M. Herrera-Hernandez, C. Aguilar-Salinas, et al. 2020. The causal effect of obesity on prediabetes and insulin resistance reveals the important role of adipose tissue in insulin resistance. *PLoS Genet.* 16:e1009018. <https://doi.org/10.1371/journal.pgen.1009018>
- Moseti, D., A. Regassa, and W.K. Kim. 2016. Molecular Regulation of Adipogenesis and Potential Anti-Adipogenic Bioactive Molecules. *Int. J. Mol. Sci.* 17:124. <https://doi.org/10.3390/ijms17010124>
- Muir, L.A., C.K. Neeley, K.A. Meyer, N.A. Baker, A.M. Brosius, A.R. Washabaugh, O.A. Varban, J.F. Finks, B.F. Zamarron, C.G. Flesher, et al. 2016. Adipose tissue fibrosis, hypertrophy, and hyperplasia: Correlations with diabetes in human obesity. *Obesity (Silver Spring).* 24:597–605. <https://doi.org/10.1002/oby.21377>
- NCD Risk Factor Collaboration (NCD-RisC). 2016. Trends in adult body-mass index in 200 countries from 1975 to 2014: a pooled analysis of 1698 population-based measurement studies with 19.2 million participants. *Lancet.* 387:1377–1396. [https://doi.org/10.1016/S0140-6736\(16\)30054-X](https://doi.org/10.1016/S0140-6736(16)30054-X)
- Négre, R., P. Grimaldi, and G. Ailhaud. 1978. Establishment of preadipocyte clonal line from epididymal fat pad of ob/ob mouse that responds to insulin and to lipolytic hormones. *Proc. Natl. Acad. Sci. USA.* 75:6054–6058. <https://doi.org/10.1073/pnas.75.12.6054>
- Park, J.-Y., Y. Kim, J.A. Im, S. You, and H. Lee. 2014. Inhibition of Adipogenesis by Oligonol through Akt-mTOR Inhibition in 3T3-L1 Adipocytes. *Evid.-Based Complement. and Alternat. Med.* 2014:1–11. <https://doi.org/10.1155/2014/895272>
- Peitz, M., K. Pfannkuche, K. Rajewsky, and F. Edenhofer. 2002. Ability of the hydrophobic FGF and basic TAT peptides to promote cellular uptake of recombinant Cre recombinase: a tool for efficient genetic engineering of mammalian genomes. *Proc. Natl. Acad. Sci. USA.* 99:4489–4494. <https://doi.org/10.1073/pnas.032068699>
- Pinnick, K.E., G. Nicholson, K.N. Manolopoulos, S.E. McQuaid, P. Valet, K.N. Frayn, N. Denton, J.L. Min, K.T. Zondervan, J. Fleckner, et al. MolPAGE Consortium. 2014. Distinct developmental profile of lower-body adipose tissue defines resistance against obesity-associated metabolic complications. *Diabetes.* 63:3785–3797. <https://doi.org/10.2337/db14-0385>
- Reichert, M., and D. Eick. 1999. Analysis of cell cycle arrest in adipocyte differentiation. *Oncogene.* 18:459–466. <https://doi.org/10.1038/sj.onc.1202308>
- Rodeheffer, M.S., K. Birsoy, and J.M. Friedman. 2008. Identification of white adipocyte progenitor cells in vivo. *Cell.* 135:240–249. <https://doi.org/10.1016/j.cell.2008.09.036>
- Ruiz-Ojeda, F.J., A.I. Rupérez, C. Gomez-Llorrente, A. Gil, and C.M. Aguilera. 2016. Cell Models and Their Application for Studying Adipogenic Differentiation in Relation to Obesity: A Review. *Int. J. Mol. Sci.* 17:1040. <https://doi.org/10.3390/ijms17071040>
- Schmidt, M., S. Fernandez de Mattos, A. van der Horst, R. Klompaker, G.J. Kops, E.W. Lam, B.M. Burgering, and R.H. Medema. 2002. Cell cycle inhibition by FoxO forkhead transcription factors involves down-regulation of cyclin D. *Mol. Cell Biol.* 22:7842–7852. <https://doi.org/10.1128/MCB.22.22.7842-7852.2002>
- Schmidt, V., N. Schulz, X. Yan, A. Schürmann, S. Kempa, M. Kern, M. Blüher, M.N. Poy, G. Olivecrona, and T.E. Willnow. 2016. SORLA facilitates insulin receptor signaling in adipocytes and exacerbates obesity. *J. Clin. Invest.* 126:2706–2720. <https://doi.org/10.1172/JCI84708>
- Schwalie, P.C., H. Dong, M. Zachara, J. Russeil, D. Alpern, N. Akhiche, C. Caprara, W. Sun, K.U. Schlaudraff, G. Soldati, et al. 2018. A stromal cell population that inhibits adipogenesis in mammalian fat depots. *Nature.* 559:103–108. <https://doi.org/10.1038/s41586-018-0226-8>
- Shao, M., L. Vishvanath, N.C. Busbuso, C. Hepler, B. Shan, A.X. Sharma, S. Chen, X. Yu, Y.A. An, Y. Zhu, et al. 2018. De novo adipocyte differentiation from Pdgfrβ⁺ preadipocytes protects against pathologic visceral adipose expansion in obesity. *Nat. Commun.* 9:890. <https://doi.org/10.1038/s41467-018-03196-x>
- Singh, A.S., C. Mulder, J.W. Twisk, W. van Mechelen, and M.J. Chinapaw. 2008. Tracking of childhood overweight into adulthood: a systematic review of the literature. *Obes. Rev.* 9:474–488. <https://doi.org/10.1111/j.1467-789X.2008.00475.x>
- Smith, P.J., L.S. Wise, R. Berkowitz, C. Wan, and C.S. Rubin. 1988. Insulin-like growth factor-I is an essential regulator of the differentiation of 3T3-L1 adipocytes. *J. Biol. Chem.* 263:9402–9408. [https://doi.org/10.1016/S0021-9258\(19\)76555-7](https://doi.org/10.1016/S0021-9258(19)76555-7)
- Smith, E.N., W. Chen, M. Kähönen, J. Kettunen, T. Lehtimäki, L. Peltonen, O.T. Raitakari, R.M. Salem, N.J. Schork, M. Shaw, et al. 2010. Longitudinal genome-wide association of cardiovascular disease risk factors in the Bogalusa heart study. *PLoS Genet.* 6:e1001094. <https://doi.org/10.1371/journal.pgen.1001094>
- Spalding, K.L., E. Arner, P.O. Westermark, S. Bernard, B.A. Buchholz, O. Bergmann, L. Blomqvist, J. Hoffstedt, E. Näslund, T. Britton, et al. 2008. Dynamics of fat cell turnover in humans. *Nature.* 453:783–787. <https://doi.org/10.1038/nature06902>
- Sun, W., H. Dong, M. Balaz, M. Slyper, E. Drokhljansky, G. Colleluori, A. Giordano, Z. Kovanicova, P. Stefanicka, L. Balazova, et al. 2020. snRNA-seq reveals a subpopulation of adipocytes that regulates thermogenesis. *Nature.* 587:98–102. <https://doi.org/10.1038/s41586-020-2856-x>
- Suryawan, A., L.V. Swanson, and C.Y. Hu. 1997. Insulin and hydrocortisone, but not triiodothyronine, are required for the differentiation of pig preadipocytes in primary culture. *J. Anim. Sci.* 75:105–111. <https://doi.org/10.2527/1997.751105x>
- Tang, W., D. Zeve, J.M. Suh, D. Bosnakovski, M. Kyba, R.E. Hammer, M.D. Tallquist, and J.M. Graff. 2008. White fat progenitor cells reside in the adipose vasculature. *Science.* 322:583–586. <https://doi.org/10.1126/science.1156232>
- Tang, X., A.M. Powelka, N.A. Soriano, M.P. Czech, and A. Guilherme. 2005. PTEN, but Not SHIP2, Suppresses Insulin Signaling through the Phosphatidylinositol 3-Kinase/Akt Pathway in 3T3-L1 Adipocytes. *J. Biol. Chem.* 280(23):22523–22529. <https://doi.org/10.1074/jbc.M501949200>
- Tomiya, K., H. Nakata, H. Sasa, S. Arimura, E. Nishio, and Y. Watanabe. 1995. Wortmannin, a Specific Phosphatidylinositol 3-Kinase Inhibitor,

- Inhibits Adipocytic Differentiation of 3T3-L1 Cells. *Biochem. Biophys. Res. Commun.* 212(1):263–269. <https://doi.org/10.1006/bbrc.1995.1965>
- Vijay, J., M.F. Gauthier, R.L. Biswell, D.A. Louiselle, J.J. Johnston, W.A. Cheung, B. Belden, A. Pramatarova, L. Biertho, M. Gibson, et al. 2020. Single-cell analysis of human adipose tissue identifies depot and disease specific cell types. *Nat. Metab.* 2:97–109. <https://doi.org/10.1038/s42255-019-0152-6>
- Wang, Q.A., C. Tao, R.K. Gupta, and P.E. Scherer. 2013. Tracking adipogenesis during white adipose tissue development, expansion and regeneration. *Nat. Med.* 19:1338–1344. <https://doi.org/10.1038/nm.3324>
- Whittle, A.J., M. Jiang, V. Peirce, J. Relat, S. Virtue, H. Ebinuma, I. Fukamachi, T. Yamaguchi, M. Takahashi, T. Murano, et al. 2015. Soluble LR11/SorLA represses thermogenesis in adipose tissue and correlates with BMI in humans. *Nat. Commun.* 6:8951. <https://doi.org/10.1038/ncomms9951>
- Zhang, P., J. Li, Y. Qi, X. Tang, J. Duan, L. Liu, Z. Wu, J. Liang, J. Li, X. Wang, et al. 2016a. Tissue Inhibitor of Matrix Metalloproteinases-1 Knock-down Suppresses the Proliferation of Human Adipose-Derived Stem Cells. *Stem Cells Int.* 2016:4761507. <https://doi.org/10.1155/2016/4761507>
- Zhang, W., S. Schmult, M. Du, J. Liu, Z. Lu, H. Zhu, S. Xue, and F. Lian. 2016b. Estrogen Receptor α and β in Mouse: Adipose-Derived Stem Cell Proliferation, Migration, and Brown Adipogenesis In Vitro. *Cell. Physiol. Biochem.* 38:2285–2299. <https://doi.org/10.1159/000445583>

Supplemental material

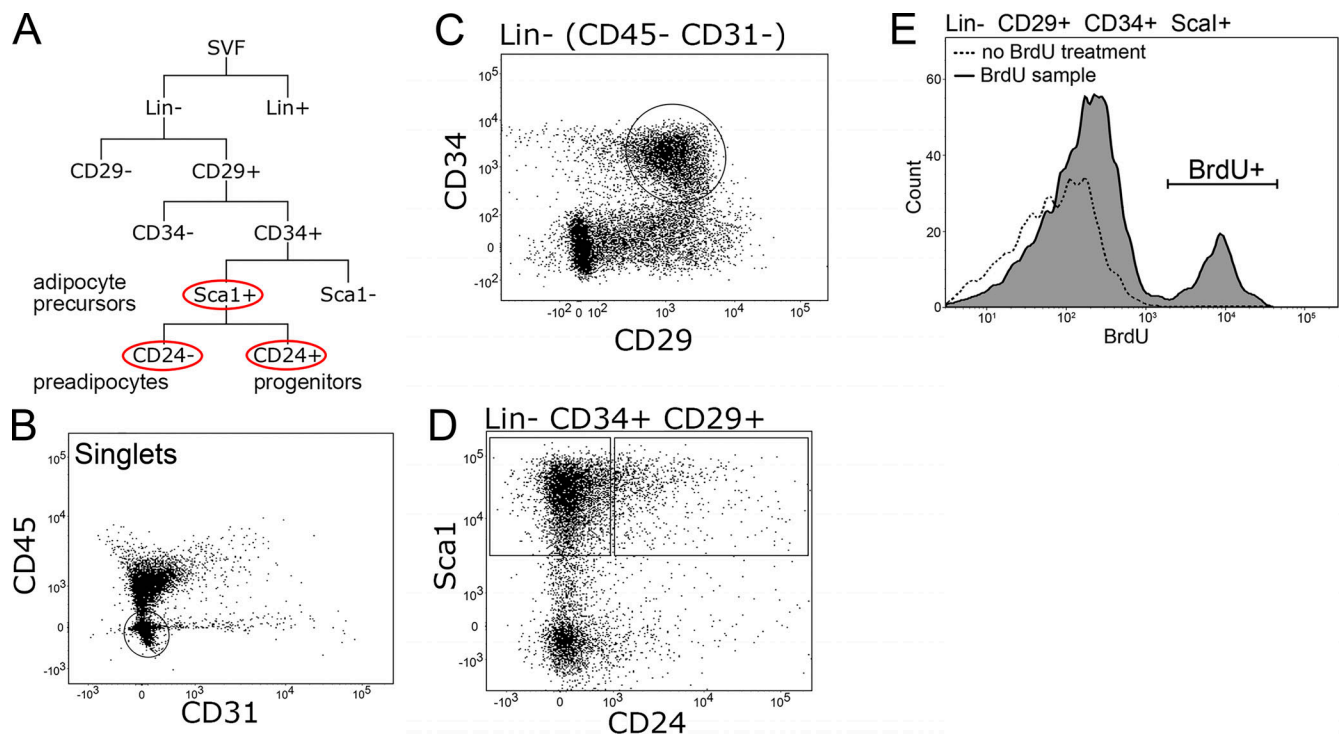


Figure S1. **Sorting of proliferating adipocyte precursor cells from murine WAT.** (A) Strategy for multicolor FACS of early adipocyte precursor cells from murine WAT (method adapted from Rodeheffer et al, 2008). Adipocyte precursors (Lin⁻CD29⁺CD34⁺Sca1⁺), consisting of early progenitors (CD24⁺) and committed preadipocytes (CD24⁻), are highlighted by red circles. (B–D) Identification of adipocyte precursors in murine epWAT. Dot blots show exemplary FACS staining profiles and gating (black boxes or circles) of the SVF from juvenile WT mice. Singlets are sorted for lack of CD31 and CD45 expression (B) and are further separated based on expression of CD34 and CD29 (C). Last, Lin⁻CD34⁺CD29⁺ cells are sorted based on expression of Sca1 (D). (E) Representative histogram showing gating for BrdU⁺ adipocyte precursors in control (no BrdU treatment) and in experimental (BrdU-treated) murine epWAT samples from WT mice.

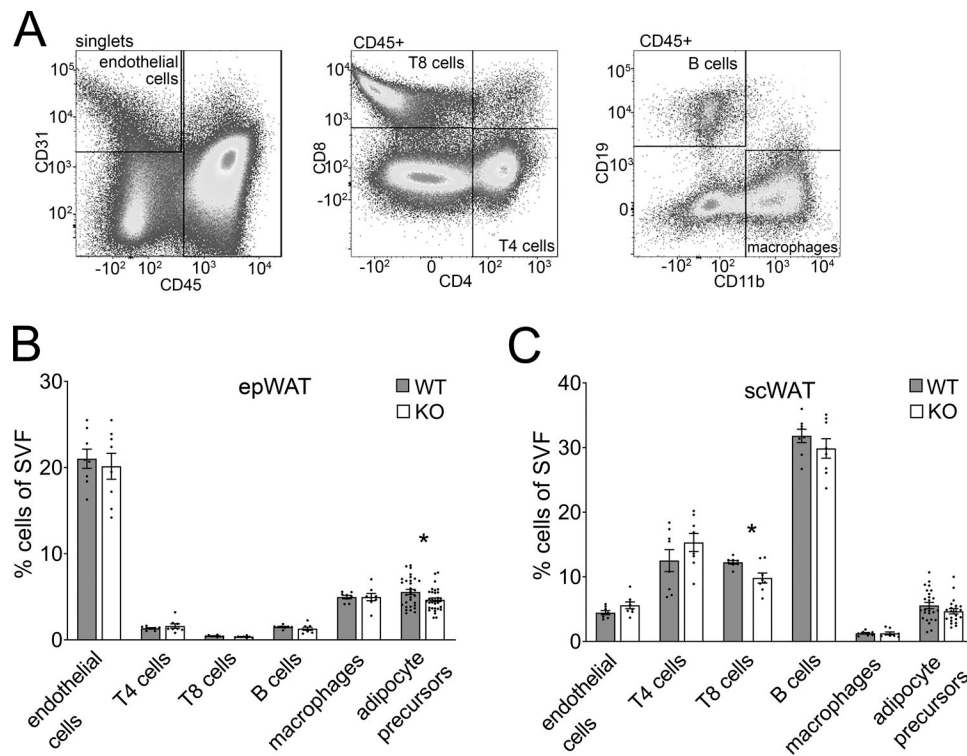


Figure S2. **Sorting of cell types from murine WAT.** (A) Exemplary FACS staining profiles and gating of various cell types in the SVF of murine ep adipose tissue. Endothelial cells (CD31⁺), T cells (CD4⁺ and CD8⁺), B cells (CD19⁺), and macrophages (CD11b⁺) are highlighted by squares. (B and C) Quantification of the various cell types in murine ep (B) and sc (C) WAT of SORLA WT and KO mice. Data are given as mean \pm SEM ($n = 7$ or 8 ; for adipocyte precursors, $n = 22-33$). Significance of data was determined using two-sided Student's *t* test; data distribution was assumed to be normal, but this was not formally tested; *, $P < 0.05$.

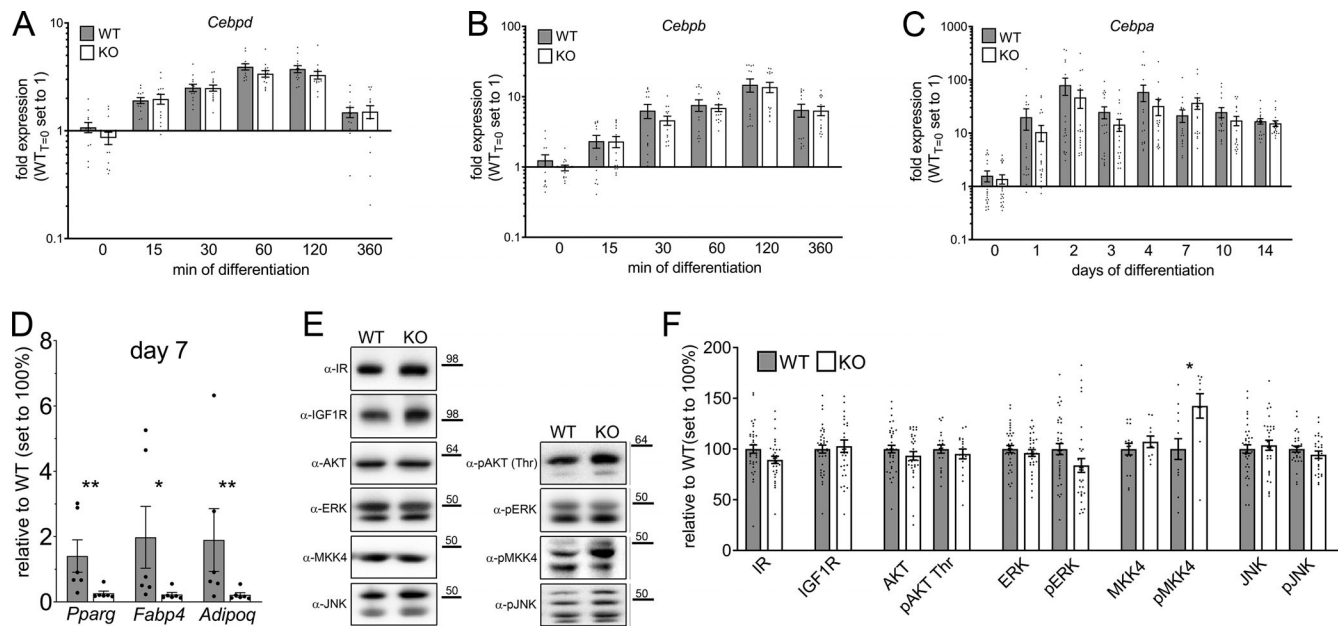


Figure S3. Adipogenic differentiation potential of MEFs from SORLA WT and KO mice. (A–C) MEFs from WT and SORLA KO mice were differentiated by treatment with induction medium and the expression of marker genes of early *Cebpd* and *Cebpb* and medial to late stages of induction *Cebpa* were tested by quantitative RT-PCR. Transcript levels are given as fold change in WT and KO cells as compared with WT cells at $t = 0$ (set to 1) as mean \pm SEM. No significant differences in gene induction levels were noted comparing genotypes ($n = 13$ – 20 individual experiments; two-way ANOVA). (D) Quantitative RT-PCR analysis of transcript levels of the indicated genes in mature adipocytes differentiated from WT and SORLA KO MEFs (day 7 of differentiation). Transcript levels are given as mean \pm SEM ($n = 6$). Statistical significance was evaluated using two-sided Mann–Whitney test; *, $P < 0.05$; **, $P < 0.01$. (E and F) Expression of the indicated proteins in untreated MEFs from WT and SORLA KO mice was determined by Western blot analyses. (E) Exemplary immunoblots. Numbers to the right of the blots are in kilodaltons. (F) The results of densitometric scanning of replicate blots ($n = 17$ – 36 independent experiments). Protein levels are given as mean \pm SEM relative to WT (set at 100%). Statistical significance was evaluated using two-sided Student's t test; *, $P < 0.05$. A normal distribution of data was assumed in A and F, but this was not formally tested.